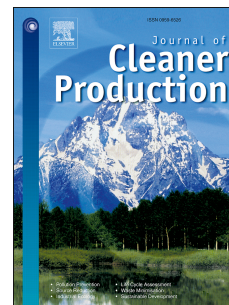


Journal Pre-proof

Energy, exergy and economic analyses of new coal-fired cogeneration hybrid plant with wind energy resource

Z.X. Li, M.A. Ehyaei, A. Ahmadi, D.H. Jamali, R. Kumar, Stéphane Abanades



PII: S0959-6526(20)32378-7

DOI: <https://doi.org/10.1016/j.jclepro.2020.122331>

Reference: JCLP 122331

To appear in: *Journal of Cleaner Production*

Received Date: 16 August 2019

Revised Date: 15 May 2020

Accepted Date: 15 May 2020

Please cite this article as: Li ZX, Ehyaei MA, Ahmadi A, Jamali DH, Kumar R, Abanades Sté, Energy, exergy and economic analyses of new coal-fired cogeneration hybrid plant with wind energy resource, *Journal of Cleaner Production* (2020), doi: <https://doi.org/10.1016/j.jclepro.2020.122331>.

This is a PDF file of an article that has undergone enhancements after acceptance, such as the addition of a cover page and metadata, and formatting for readability, but it is not yet the definitive version of record. This version will undergo additional copyediting, typesetting and review before it is published in its final form, but we are providing this version to give early visibility of the article. Please note that, during the production process, errors may be discovered which could affect the content, and all legal disclaimers that apply to the journal pertain.

© 2020 Published by Elsevier Ltd.

1 **Energy, exergy and economic analyses of new coal-fired cogeneration hybrid plant with wind energy**
2 **resource**

3 **Z.X.Li^{(1), (2)}, M.A. Ehyaei^{(3)*}, A. Ahmadi⁽⁴⁾, D. H. Jamali⁽⁵⁾, R. Kumar⁽⁶⁾, Stéphane Abanades⁽⁷⁾**

4 1. School of Engineering, Ocean University of China, Tsingdao 266100, China

5 2. School of Mechanical, Materials, Mechatronic and Biomedical Engineering, University of Wollongong,
6 Wollongong, NSW 2522, Australia

7 3. Department of Mechanical Engineering, Pardis Branch, Islamic Azad University, Pardis New City, Iran

8 4. Iran University of Science and Technology, School of New Technologies, Department of Energy
9 Systems Engineering, Iran

10 5. School of Environment, College of Engineering, University of Tehran, Tehran, Iran

11 6. School of Mechanical Engineering, Lovely Professional University, Phagwara, Punjab, India

12 7. Processes, Materials, and Solar Energy Laboratory, PROMES-CNRS, 7 Rue du Four Solaire, 66120 Font-
13 Romeu, France

14 ***Corresponding author: E-mail: aliehyaei@yahoo.com, Tel: +98-9123478028**

15 **Abstract.** A novel configuration of a coal-fired cogeneration plant is proposed in this paper. This novel
16 system is composed of combustion chamber, Rankine cycle, absorption chiller, alkaline electrolyzer, and
17 methanation plant. In the proposed configuration, the heat of exhaust gas from the combustion
18 chamber can be used in a Rankine cycle to produce electricity. The heat of exhaust gas also powers the
19 absorption chiller to provide cooling. The exhaust gas flows through a sulfur extraction unit to separate
20 sulfur from CO₂ gas. To supply electrical power, wind turbines alongside the Rankine cycle are
21 considered. A part of the produced electricity from both the Rankine cycle and the wind turbines can be
22 used by an alkaline electrolyzer to produce hydrogen and oxygen. The CO₂ gas from sulfur unit and

23 hydrogen gas (H_2) provided by the electrolyzer can be delivered to a methanation unit to produce syngas
24 (CH_4) for different applications. The oxygen from the electrolyzer is injected into the combustion
25 chamber to improve the combustion process. Results show that by using 80 units of 1 MW Nordic wind
26 turbine to generate electricity, all of the CO_2 in the exhaust gas is converted to syngas. The whole
27 system energy and exergy efficiencies are equal to 16.6% and 16.2%. The highest and lowest energy
28 efficiencies of 85% and 30.1% are related to compressor and steam power plants. The energy and exergy
29 efficiencies of the wind turbine are 30.7 % and 11.9 %. The system can produce 40920.4 MWh of
30 electricity and 180.5 MWh of cooling. As CO_2 is consumed to produce syngas, the proposed system is
31 capable of avoiding a significant amount of 2776 t CO_2 emissions while producing 1009.4 t syngas
32 annually. Based on economic analysis, the payback period of the system is 11.2 y, and internal rate of
33 return is found to be 10%, which can prove the viability of the proposed configuration.

34
35 **Keywords:** Energy, Exergy, Power to gas, Methanation, Rankine cycle, Wind turbine

36

37 1. Introduction

38 The worldwide energy demand for electricity generation is growing steadily. Fossil fuel is playing a major
39 role to fulfill this demand. The excessive use of fossil fuel within the current energy infrastructure is
40 causing natural disasters and health issues. The continuous CO_2 emissions are at least partially
41 responsible for global warming (Atabi et al., 2014; Mozafari and Ehyaei, 2012). In 2016, coal-based
42 power plants and other carbon-intensive sectors for electricity and heat generation contributed to 42%
43 of global emissions (Shirmohammadi et al., 2018). By 2040, it is expected that global energy-related
44 carbon dioxide emissions may reach around 43.2 billion t (Conti et al., 2016). These considerable global
45 emissions are forcing policymakers to adopt an eco-friendly and sustainable alternative option for
46 power generation in the entire world. Renewable Energy (RE) sources may play a key role to achieve this
47 target because of their environmentally-friendly nature. Solar and wind energy resources are playing a

48 crucial role in electricity generation while shifting fossil fuel consumption towards cleaner energy
49 sources (Dorotić et al., 2019; Shaygan et al., 2019). According to an estimate, RE sources contribution to
50 power supply was estimated to be more than 30% during 2010-2015 (Bellocchi et al., 2019). The impact
51 of implementing RE sources in the heat and transportation sector is attracting more attention due to the
52 dependency of this sector on fossil fuels (Dorotić et al., 2019). The European Commission target
53 included 20% of RE contribution in its 2021 energy roadmap (Roadmap, 2011). Amongst various RE
54 resources, the wind power promises a great potential in electricity generation and it reached up to 539
55 GW in 2017 globally. Hydrogen is also a promising viable option to replace fossil fuels for reliable power
56 generation and for being used as vehicles fuel. The main advantage of hydrogen as an energy carrier is
57 its flexible conversion into other energy forms in an efficient way in comparison to fossil fuels
58 (Castaneda et al., 2013; Li et al., 2019).

59 Due to rapid growth in gas-fired based electricity generation, the integration of electricity, district
60 heating and RE resources are attracting research towards clean energy generation in recent years.
61 Researchers are also focusing on wind-solar hybrid power plants and trying to integrate different
62 energy carriers in an energy hub (Gholizadeh et al., 2019; Yang et al., 2018). It has been proven that
63 multi-products system can significantly enhance the performance of the system in comparison to single-
64 product system (Jamali and Noorpoor, 2019; Li et al., 2019). The rules and regulations set by
65 international organizations to mitigate climate changes are forcing the nations to promote clean energy
66 (Lisbona et al., 2018).

67 The search for innovative technologies framework for sustainable development is getting more
68 importance in the energy sector in recent years. Power-to-gas (PtG) technique is a viable option for the
69 storage of surplus electricity generated by RE sources. It is a rising technology in the future energy
70 sector to compete with existing technologies used for power generation (Walker et al., 2017; Weidner et
71 al., 2018). In PtG, gas fuel is produced and long-term stored using electricity. The main advantage of this

72 technology is that the surplus electricity is absorbed from the grid. Wind and solar power have great
73 potential for the long term PtG operation (Guandalini et al., 2017). The use of an electrolyzer provides
74 hydrogen from the electricity (Kreuter and Hofmann, 1998). There are various types of electrolysis
75 technologies such as high-temperature electrolysis, alkaline water electrolysis, and polymer electrolyte
76 electrolysis that are developed worldwide at large, laboratory and small scale (Buttler and Spliethoff,
77 2018). The separated pure hydrogen along with captured CO₂ can be used directly in the methanation
78 process to produce Synthetic Natural Gas (SNG) (Ghaib and Ben-Fares, 2018). This gas can be used as a
79 carbon-neutral fuel in the transport sector to reduce the level of CO₂ emissions. Another research was
80 carried out to compare different catalysts usually used for CO₂ methanation. The catalysts were tested
81 to determine the most suitable operating temperature and pressure, which turned out to be 673 K and
82 10 bar (García-García et al., 2018).

83 PtG systems proved to be suitable for sustainable energy storage using renewable energy sources
84 (Lewandowska-Bernat and Desideri, 2018; Llera et al., 2018). Several studies on PtG plant have also
85 been performed in recent years. PtG projects in Europe have been reviewed and discussed in detail
86 (Wulf et al., 2018). PtG and Power to liquid (PtL) were identified as promising concepts to avoid source
87 fluctuations when renewable energies are considered as primary energy sources. The CO₂ reduction
88 trends were predicted in the case of using these technologies, and biomass gasification with subsequent
89 hydrogenation could have great performance in integration with PtG systems (Bellocchi et al., 2019).
90 Schaaf et al. (2014) proposed a system to store excess electricity produced from renewable sources such
91 as solar and wind power plants and to use this electricity to provide hydrogen for the methanation with
92 CO₂. In another study, a retrofit unit was integrated into a gas turbine plant for methanation purposes.
93 In that system, the CO₂ was extracted from flue gas of the gas turbine plant, and hydrogen was provided
94 from water electrolysis to produce methane (Boubenia et al., 2017). Direct methanation of flue gas was
95 proposed using renewable hydrogen production by Laquaniello et al.(2018). The integration of hydrogen

96 in PtG networks was assessed to find out its effect on the natural gas pipelines infrastructure (Gondal,
97 2019). A study focused on efficiency enhancement of a Sabatier-based PtG system by pinch analysis
98 method, which revealed the significant potential of this concept. By thermoeconomic and sensitivity
99 analysis, the critical components of the plant were highlighted (Toro and Sciubba, 2018). A system to
100 integrate biogas plant to a membrane-based PtG system was also proposed. Two different processes for
101 methanation were compared to study their feasibility (Kirchbacher et al., 2018). Applications of PtG
102 were studied by retrofit plants in building energy systems through three different configurations (De
103 Santoli et al., 2017). The impact of curtailment of wind-based generation on PtG was performed and the
104 results showed that the impact of the activity was positive (Gholizadeh et al., 2019). A hybrid technology
105 using PtG-biomass was reported to be most suitable in process industries (Bailera et al., 2016). Several
106 studies have shown substantial cost reduction for methanation process and electrolysis, and this trend
107 should continue until 2050 (Thema et al., 2019). Thermo-economic analysis of Sabatier based PtG plant
108 was achieved to enhance plant efficiency (Toro and Sciubba, 2018). Thermodynamic, economic and
109 environmental analyses were performed and showed promising results considering that water
110 electrolysis will experience investment cost reduction (Boubenia et al., 2017). In another research, a 100
111 MW PtG was proposed and analyzed from an economic point of view, in which the system used solid
112 oxide cell to both produce hydrogen and to use it reversibly for electricity generation when power is
113 lacking (Miao and Chan, 2019). In a study, a gas turbine, an air bottoming cycle and a steam reforming
114 unit were integrated for electricity and hydrogen production (Ahmadi et al., 2020). They found that
115 adding steam reforming unit to the integrated gas and air bottoming cycles could enhance the energy
116 and exergy efficiencies, and this combination would be advantageous from economic and environmental
117 aspects.

118 The previous studies conclude that the utilization of carbon dioxide in syngas production is highly
119 required because of the lower impact during combustion. In the present study, an integrated new

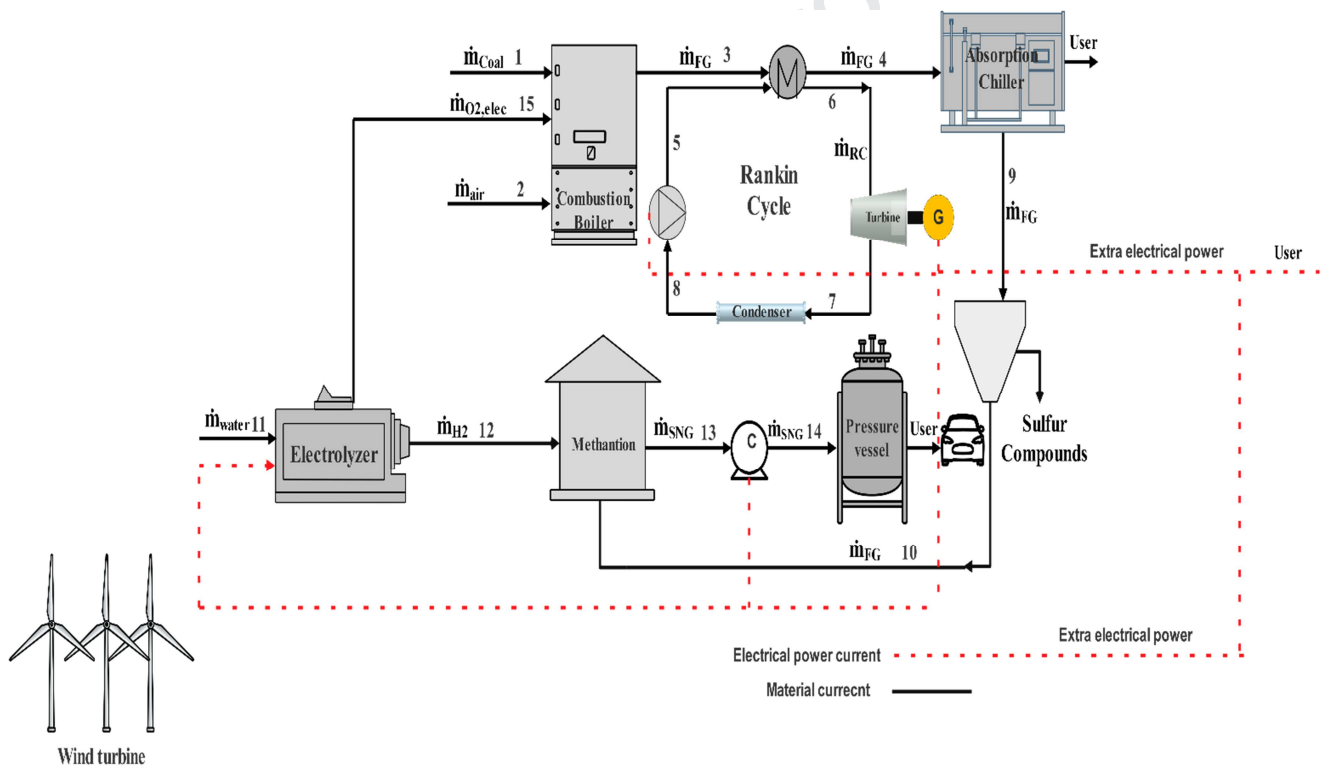
120 system configuration using electricity from steam cycle and wind power plant along with gas through
121 oxy-fuel combustion unit to produce syngas has been investigated. Thermal performance analysis of the
122 plant has been performed in this study. The entire plant is a complex system due to the number of
123 components working simultaneously in parallel and in series combination. This new system with such
124 configuration has never been proposed so far. In this novel configuration, in the burner, coal is burned
125 with air to produce hot gas. Hot gas energy is recovered in the Rankine cycle and absorption chiller to
126 produce electricity and cooling. Sulfur components are removed from the exhaust gas and CO₂ is
127 reacted with hydrogen in the methanation plant to produce syngas (CH₄). This syngas is pressurized
128 with compressor and stored in the pressure vessel. The syngas produced at the outlet of the plant can
129 be compressed and utilized for vehicles as a fuel. Energy and exergy analyses of individual components
130 of the proposed plant have been proposed. The electrical power consumption of the system
131 components matches the electricity produced by both the Rankine cycle and wind turbine. The novelties
132 of this study are the proposal of an integrated new configuration of power to gas cycle with energy
133 recovery of exhaust hot gas from the boiler. The reduction of a large portion of CO₂ emissions via
134 conversion to syngas by using wind energy is an important aspect, which is highly desirable to reduce
135 environmental pollution in present situation. Sensitivity analysis of the main parameters of this system is
136 performed to evaluate the impact of several decision variables on the system performance.

137 **2. Mathematical modeling**

138 **2.1. Process description**

139 The schematic diagram of the system is shown in Figure 1. In this system, coal (point 1) is reacted with
140 air (point 2) and oxygen produced in the electrolyzer (point 15) to produce hot flue gas (FG) (point 3).
141 Hot flue gas supplies the energy needs (points 3 and 4) of the evaporator of the Rankine Cycle (RC) to
142 produce electricity by superheat organic working fluid (points 5 and 6). It is passed through absorber of
143 absorption chiller (points 4 and 9) to produce cooling. After removing sulfur compounds (point 10), the

144 flue gas is reacted with hydrogen supplied by the electrolyzer (point 12) to produce syngas (CH_4) point
 145 13. Produced syngas (point 13) is pressurized in the compressor (point 14) and it is stored in the
 146 pressure vessel for various applications. The electricity needs of compressor and electrolyzer are
 147 supplied by the electrical production of the wind turbine and Rankine cycle (steam power plant).
 148 Extra electrical power production can be used by the user. The fuel of this system is coal and the outputs
 149 are cooling produced by absorption chiller, electrical power produced by both Rankine cycle and wind
 150 turbine, and syngas product.



151

Wind turbine

152

Figure1. Schematic diagram of the system

153 The considered assumptions in this model are as follows:

154

1- The system is at steady state.

155

2- Initial state condition is 15°C and 1 atm.

- 156 3- Combustion boiler efficiency is 0.92.
- 157 4- The process in the pump and turbine is polytropic.
- 158 5- For the wind speed, the Weibull distribution density function is considered to calculate the
159 power production by the wind turbine.
- 160 6- The polytropic efficiencies of the pump, turbine, and compressor are 0.85.
- 161 7- Pressure loss is assumed to be 2%.
- 162 8- Flue gas loss is assumed to be 3%.
- 163 9- Evaporator and condenser heat transfer efficiencies are assumed to be 90%.

164 2.2. Mass and energy balances

165 Based on the ultimate analysis of coal, the needs of oxygen and air mass flow rate for coal combustion
166 are calculated by (Bailera et al., 2015):

$$\dot{m}_{O_2} = \dot{m}_{Coal} r_a (2.667x_C + (8x_H - x_O) + x_S) \quad (1)$$

$$\dot{m}_{air} = 4.32 \dot{m}_{Coal} r_a (2.667x_C + (8x_H - x_O) + x_S) \quad (2)$$

167 In equation 1, the parameter x is the weight fraction, C, H, O and S denote carbon, hydrogen, oxygen
168 and sulfur, r_a represents air fuel ratio.

169 The alkaline electrolyzer is used to split water into hydrogen and oxygen. In general, the reaction
170 presented by equation 3 takes place in the electrolyzer (Tijani et al., 2014; Ulleberg, 2003):



171 The operating voltage in each cell of the electrolyzer is calculated by (Tijani et al., 2014; Ulleberg, 2003):

$$V_{cell} = V_{rev} + V_{act} + V_{ohm} \quad (4)$$

172 In equation 4, subscripts rev, act and ohm denote reversible, activation and ohmic. The calculation
173 equations for V_{rev} , V_{act} and V_{ohm} are presented in Table 1 (Tijani et al., 2014; Ulleberg, 2003).

174

175

176

Table 1. Calculation equations for V_{rev} , V_{act} and V_{ohm}

No	Parameter	Equation
1	V_{rev}	$\frac{\Delta G}{2F}$
2	V_{act}	$S \log \left(\frac{(t_1 + \frac{t_2}{T_{elec}} + \frac{t_3}{T_{elec}}) I}{A} + 1 \right)$
3	V_{ohm}	$\frac{(r_1+r_2) T_{elec}}{A}$

177

178 In Table 1, ΔG is the Gibbs energy (237.2 kJ/mol), F is the Faraday's constant (96495 C/mol), A is the
 179 area of the electrode, I is the current, r_1 and r_2 are the ohmic resistance parameters, t_1 , t_2 , and t_3 are
 180 the electrode overvoltage coefficients.

181 The current efficiency of alkaline electrolyzer can be expressed as follows (Tijani et al., 2014; Ulleberg,
 182 2003):

$$\eta_F = \frac{\left(\frac{I}{A}\right)^2}{f_1 + \left(\frac{I}{A}\right)^2} f_2 \quad (5)$$

183 In equation 5, f_1 and f_2 are the parameters related to electrolyzer and Faraday efficiencies.

184 Hydrogen production mass flow rate in alkaline electrolyzer is calculated by (Tijani et al., 2014; Ulleberg,
 185 2003):

$$\dot{m}_{H_2} = \eta_F N_{cell} \frac{I}{F} \quad (6)$$

186 In equation 6, N_{cell} is the number of cells.

187 The power consumption in alkaline electrolyzer is calculated by (Tijani et al., 2014; Ulleberg, 2003):

$$\dot{W}_{elec} = N_{cell} V_{cell} \quad (7)$$

188 In the methanation plant, the reaction presented by equation 8 takes place (Bailera et al., 2015):



189 The purity of CO₂ has a significant impact on methanation efficiency. The considered CO₂ capture
190 technology is chemical absorption using amines (mono-ethanolamine, MEA).

191 For the wind turbine, the average electrical generated power is obtained by (Powell, 1981):

$$\dot{W}_{wind,ave} = \dot{W}_{wind,er} \left[\frac{\exp(-(\frac{u_c}{C})^K) - \exp(-(\frac{u_r}{C})^K)}{(\frac{u_r}{C})^K - (\frac{u_c}{C})^K} - \exp(-(\frac{u_f}{C})^K) \right] \quad (9)$$

192 In equation 9, P_{er} is the rated power, u_c , u_r and u_f are cut-in rated and furling speeds. K , C are
193 parameters which are calculated by (Johnson, 2006; Justus, 1978):

$$K = \left(\frac{\sigma}{\bar{u}}\right)^{-1.086} \quad (10)$$

$$C = \frac{\bar{u}}{\Gamma\left(1 + \frac{1}{K}\right)} \quad (11)$$

194 In equation 11, \bar{u} denotes the average wind speed, Γ is the Gamma function and σ is the standard
195 deviation.

196 The system component energy and mass balances, as well as energy efficiency equations, are shown in
197 Table S1 in appendix section.

198 The number of wind turbines required to meet the system power consumption can be calculated by:

$$KK = \left[\frac{\dot{W}_{elec} + \dot{W}_c + \dot{W}_p - \dot{W}_T}{\dot{W}_{windturbine,ave}} \right] + 1 \quad (12)$$

199

200 The brackets ([]) mean integer function.

201 System energy efficiency can be calculated by:

$$\text{energy efficiency} = \frac{\dot{m}_{13} \text{LHV}_{\text{CH}_4} + \text{KK} * \dot{W}_{\text{windturbine,ave}} + \dot{Q}_{\text{abs}} + \dot{W}_{\text{T}} - \dot{W}_{\text{C}} - \dot{W}_{\text{P}}}{\dot{m}_1 \text{LHV}_{\text{CH}_4} + \text{KK} \dot{W}_{\text{windturbine,er}}} \quad (13)$$

202 2.3. Exergy balance

203 Exergy is defined as the amount of work obtainable when some matter is brought to thermodynamic
204 equilibrium with its surroundings. The total exergy consists of four components including kinetic exergy,
205 potential exergy, physical exergy and chemical exergy (Bejan, 2016).

206 ex is the total specific exergy, calculated as (Bejan, 2016):

$$\text{ex} = (h - h_0) - T_0(s - s_0) + T_0 \sum x_i R \ln y_i + \sum x_i \text{ex}_{\text{chi}} + \frac{V^2}{2} + gz \quad (14)$$

207 In equation 14, h is the enthalpy, s is the specific entropy, R is the specific gas constant, ex_{chi} is the
208 component specific chemical exergy, xi is the mass fraction, yi is the molar fraction. V is the velocity; g is
209 the gravitational acceleration and z is the height. The notation "0" is the reference state condition
210 (1atm, 288K).

211 For each component of the system, equations of exergy destruction rate and exergy efficiency are
212 shown in Table S2 in appendix section.

213 System exergy efficiency can be calculated as:

$$\text{exergy efficiency} = \frac{\dot{m}_{13} \text{ex}_{\text{ch,Ch}_4} + \text{KK} * \dot{W}_{\text{windturbine,ave}} + \dot{Q}_{\text{abs}} \left(1 - \frac{T_0}{T_{\text{abs}}}\right) + \dot{W}_{\text{T}} - \dot{W}_{\text{C}} - \dot{W}_{\text{P}}}{\dot{m}_1 \text{ex}_1 + \frac{8}{27} \rho A_2 U^3} \quad (15)$$

214 System exergy destruction is calculated by the summation of system component exergy destructions.

215 2.4. Economic analysis

216 The total investment cost represented as C_0 is obtained by the equation 16 (Bellos et al., 2019; Tzivanidis
217 et al., 2016):

$$C_0 = K_{\text{Wind turbine}} + K_{\text{Absorption chiller}} + K_{\text{Methanation}} + K_{\text{Elec}} + K_{\text{RC}} + K_{\text{Compressor}} \quad (16)$$

218 In equation 16, subscripts elec defines electrolyzer component, and K denotes the investment cost of a
219 component. The operation and maintenance costs are considered at 3% of the initial cost. For the
220 proposed system, yearly income cash flow denoted as CF is expressed as follows (Bellos et al., 2019;
221 Tzivanidis et al., 2016):

$$CF = Y_{\text{electrical}}k_{\text{electrical}} + Y_{\text{cooling}}k_{\text{cooling}} + Y_{\text{CH}_4}k_{\text{CH}_4} - Y_{\text{CO}_2}k_{\text{CO}_2} - Y_{\text{Coal}}k_{\text{Coal}} \quad (17)$$

222 In equation 17, $Y_{\text{electrical}}$, Y_{cooling} , Y_{CH_4} are productions of electrical, cooling, and syngas for a year .
223 Y_{CO_2} is carbon dioxide consumption in methanation plant for a year. Y_{Coal} is coal consumption in a year.
224 $k_{\text{electrical}}$, k_{cooling} , k_{CH_4} , k_{Coal} are the prices of electrical, cooling, syngas and coal, k_{CO_2} is a carbon tax.
225 For the investment, the Internal Rate of Return (IRR) is determined by (Bellos et al., 2019; Tzivanidis et
226 al., 2016):

$$IRR = \frac{CF}{C_0} \left[1 - \frac{1}{(1 + IRR)^N} \right] \quad (18)$$

227 Net Present Value (NPV) represents the total investment gain during the life time of the project that can
228 be expressed as (Bellos et al., 2019; Tzivanidis et al., 2016):

$$NPV = -C_0 + CF \frac{(1 + r)^N - 1}{r(1 + r)^N} \quad (19)$$

229 In equation 19, r and N denote discount factor and project lifetime that are considered to be 3% and 25
230 y. The Simple Payback Period (SPP) is calculated as follows (Bellos et al., 2019; Tzivanidis et al., 2016):

$$SPP = \frac{C_0}{CF} \quad (20)$$

231 The Payback Period (PP) equation is as follows (Bellos et al., 2019; Tzivanidis et al., 2016):

$$PP = \frac{\ln\left(\frac{C_F}{C_F - r \cdot C_0}\right)}{\ln(1 + r)} \quad (21)$$

232 Each index is independent of another one, which makes them significant individually. The initial cost
 233 functions and values are presented in Table S3 in appendix section.

234 3. Results and discussion

235 For mathematical modeling, a computational program was written in MATLAB software. This program is
 236 divided into one main program and two functions for calculating the fluid properties and wind turbine
 237 power production.

238 3.1. System specification

239 The ultimate analysis of coal is shown in Table 2 (Verma et al., 2010).

240 Table 2. Ultimate analysis of coal (weight based)

x_C	x_H	x_O	x_N	x_S	x_M	x_Z
65.72	5.27	7.1	1.29	1.69	8.09	10.84

241

242 The type of wind turbine is Nordic wind turbine with 1000 kW rated power. Specification of this wind
 243 turbine is shown in Table 3.

244 Table 3. Nordic wind turbine specification

No	Parameter	Unit	Value
1	$\dot{W}_{windturbine,er}$	kW	1000
2	u_C	m/s	4
3	u_r	m/s	16

4	u_f	m/s	22
5	h	m	70
6	A	m ²	2732

245

246 The system specification is shown in Table 4. The wind velocity value at a certain speed for Tehran is

247 shown in Table S4 in the appendix section (Atabi et al., 2014).

248

Table 4. System specification

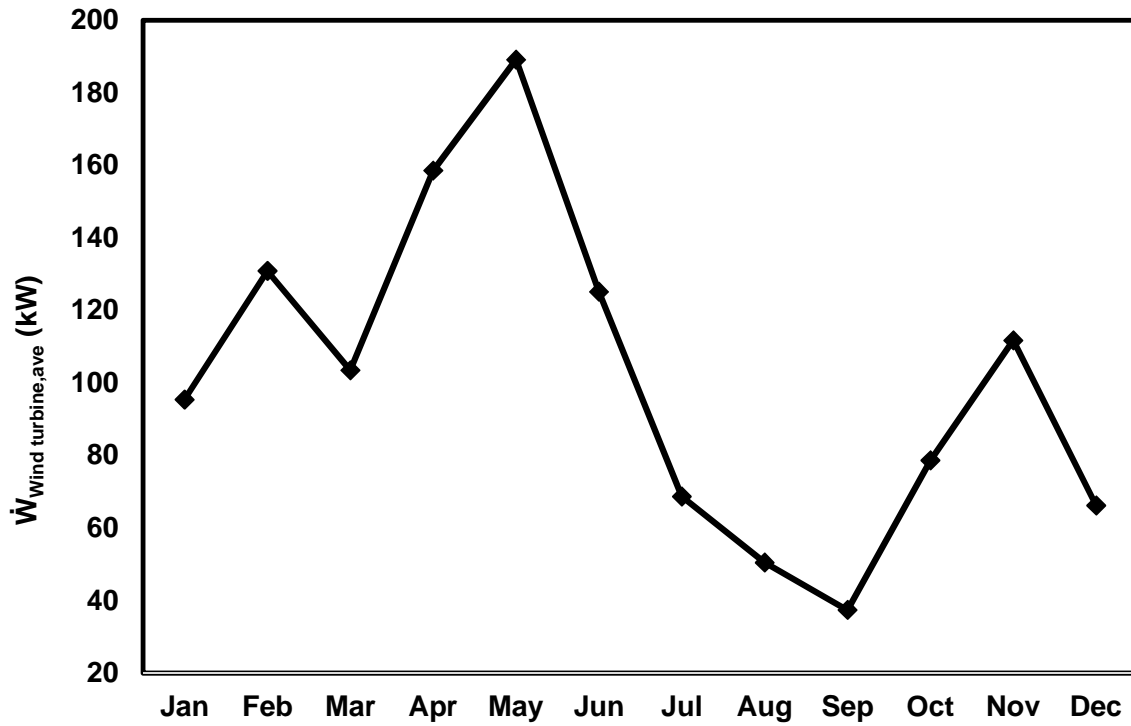
No	Parameter	Unit	Value
1	\dot{m}_1	kg/s	0.04
2	r_a	Molar basis	2.34
3	LHV _{coal}	kJ/kg	27213
4	T _{elec}	K	353.15
5	T ₁	K	288.15
6	T ₂	K	288.15
7	T ₄	K	368.15
8	T ₆	K	1324.1
8	T ₉	K	338.15
9	P ₅	kPa	8104
10	P ₆	kPa	8104
11	P ₇	kPa	40.5
11	P ₈	kPa	40.5
11	T _{pinch}	oC	30

12	η_{CC}	-	0.92
13	η_C	-	0.9
14	η_E	-	0.9
15	η_T	-	0.85
16	η_P	-	0.85
17	η_{Com}	-	0.85
18	COP	-	0.87
19	r_C	-	8
20	\dot{m}_{RC}	kg/s	0.1817

249

250 In Tables 3 & 4, r_a is the air-fuel ratio (mass basis), T_{pinch} is the temperature difference between hot gas
 251 and superheated steam, η_{CC} represents the combustion chamber efficiency. η_T , η_P , and η_C are turbine,
 252 pump and compressor polytropic efficiencies, COP defines the absorption chiller coefficient of
 253 performance, r_c is the compression factor of compressor, $\dot{W}_{windturbine,er}$ is the rated power of wind
 254 turbine, u_c , u_r and u_f are cut-in, rated and furling speeds of the wind turbine, h is the tower height of
 255 the wind turbine and A is the swept area wind turbine.

256 Figure 2 shows the monthly average wind turbine electrical power production during one year.



257

258 Figure 2. Monthly average wind turbine electrical power production during various months of a year

259 Table 5 shows the main system parameters calculated by the program.

260

Table 5. Results of the main parameters

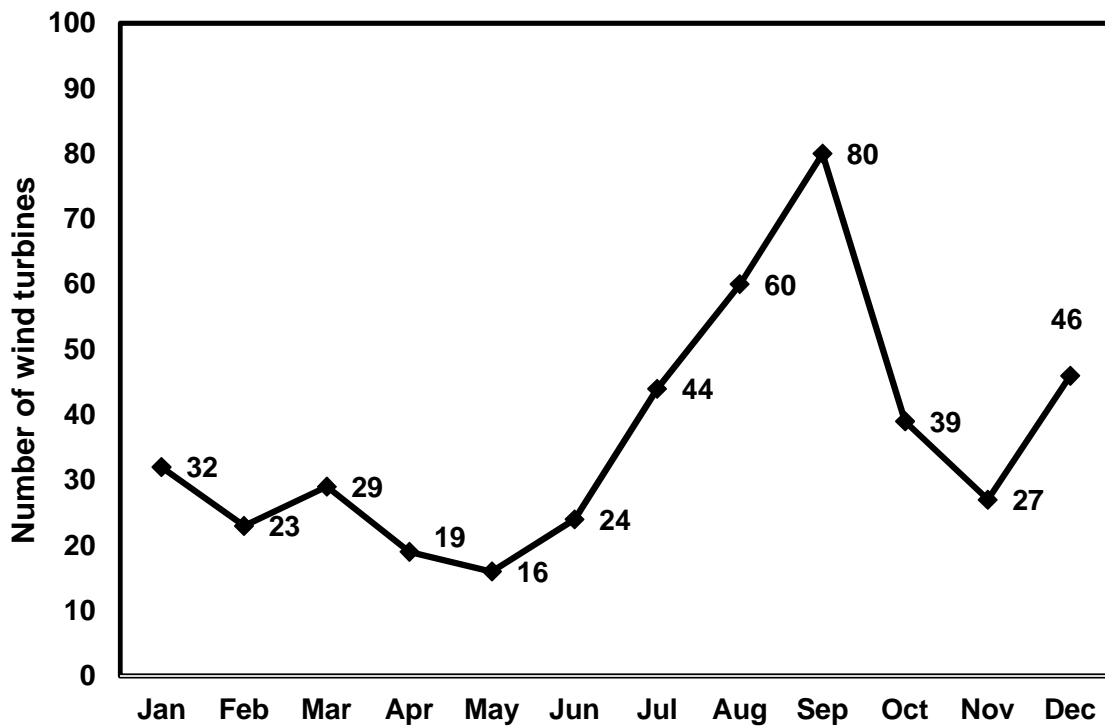
No.	Parameter	Unit	Value
1	\dot{W}_{elec}	kW	3214.2
2	\dot{W}_P	kW	1.65
3	\dot{W}_T	kW	243.4
4	\dot{W}_C	kW	16.2
5	\dot{Q}_{abs}	kW	22.6

261

262 Based on equation 12, Table 3, and Figure 2, the required number of Nordic wind turbine units is shown

263 in Figure 3. According to Figure 3, the maximum number of wind turbines needed in September is equal

264 to 80. Since the conversion of all the carbon dioxide in flue gas is guaranteed by this system, the total
 265 number of 80 of 1 MW Nordic wind turbine units is selected. For the other months of a year, the extra
 266 electrical power production can be delivered to electrical network.



267

268

Figure 3. Required number of the Nordic wind turbine units

269 Table 6 shows the system comparison with and without syngas production during a year. Power for
 270 syngas production system is required in electrolyzer, compressor, and methanation plant. The
 271 consumption of electrical power to produce syngas is calculated to be equal to 25.6 MWh/t.

272

Table 6. System comparison with and without syngas production

No.	Parameter	Unit	Value	
			With syngas	Without syngas
1	\dot{m}_{CO_2} consumption	t/y	2776	0
2	\dot{m}_{H_2} consumption	t/y	504.7	0

3	\dot{m}_{Coal} consumption	t/y	1152	1152
4	\dot{m}_{syngas} production	t/y	1009.4	0
5	\dot{Q}_{abs} cooling production	MWh	180.5	180.5
6	electrical power production	MWh	40920.4	66763.1

273

274 **3.2. Validation of theoretical model**

275 Since a similar complex system has not been investigated yet, the validation of the whole system is
 276 impossible. Each of the main components is validated individually. The average power production of the
 277 Nordic wind turbine is compared with the manufacturer power curve shown in Ref. (Pierrot, 2019).

278 Regarding wind velocity information of Tehran (province of Iran) shown in Table S4, the annual average
 279 power produced by the Nordic model wind turbine is calculated to be 103.1 kW by equation 9 while it is
 280 94.3 kW by power curve. The error is around 8%, which can be due to the following reasons:

281 1) Equation 9 uses the statistical data of the wind turbine while the power curve is based on production
 282 power versus wind velocity.

283 2) The height of the tower is not determined in Ref. (Pierrot, 2019) and it is between 60 to 70 m, which
 284 has an effect on the power produced by the wind turbine.

285 3) For the power curve, the air density is considered to be 1.225 kg/m^3 , while this value may differ for
 286 Tehran

287 For the alkaline electrolyzer, the theoretical model used in this study was validated before (Ulleberg,
 288 2003). Figures 6 to 10 of this reference were compared to the simulation and experimental data. For
 289 example, in Figure 7 of this reference, the root means square (RMS) error for hydrogen production is
 290 $0.053 \text{ Nm}^3/\text{hr}$ (in the range of 1 to 3 Nm^3/hr hydrogen production).

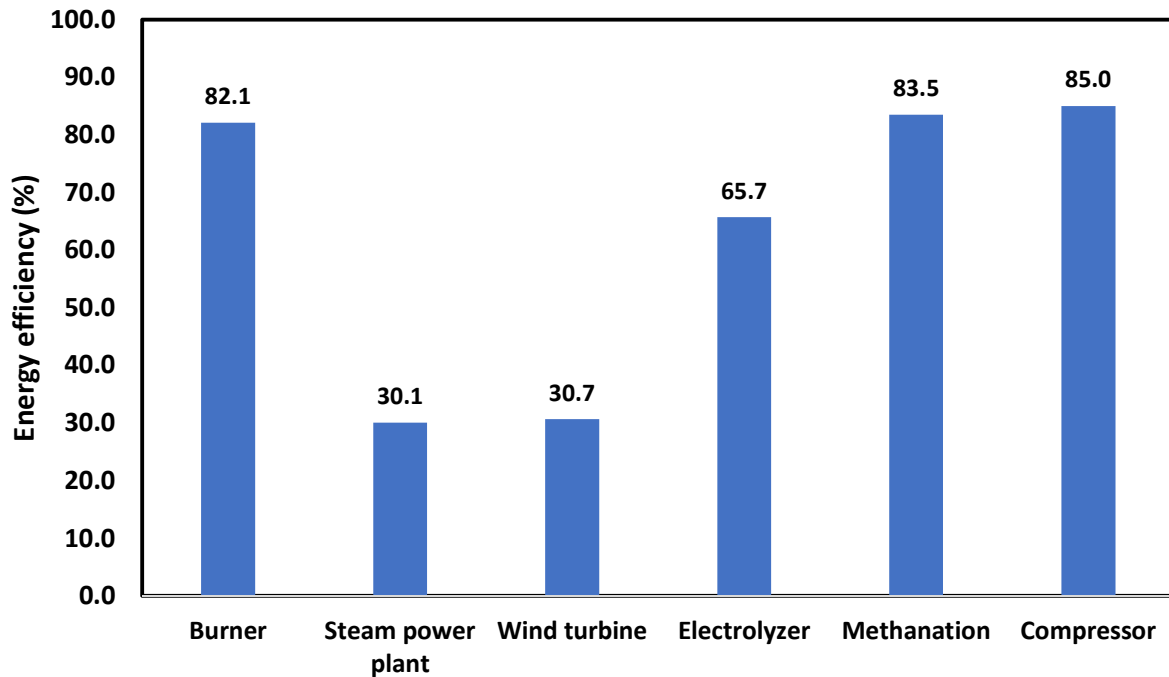
291 For validation of the combustion chamber, the exhaust gas temperature was compared with Ref.
292 (Anderson). In this reference, the process flow diagram (PFD) of one real coal-fired steam power plant is
293 given. The hot exhaust gas temperature is determined to be 1259.2 °C. By inserting the fuel and air
294 ratios to computational code, this temperature is calculated to be 1324.6 °C. The error is about 4.9%.
295 The main reasons for this error are as follows:

- 296 1) The coal composition is not specified and may be different
- 297 2) The distribution of the coal and air is different in the combustion chamber and the combustion
298 is not uniform in real conditions

299 The plant energy efficiency in that reference is about 35.2%, while it is about 30.1% in this study and the
300 mean error is about 14% because of the lack of information about the main parameters in that
301 reference. The steam turbine used in that reference has three stages (i.e., high, medium and low
302 pressure steam), while the one stage steam turbine is considered in this study. The pure oxygen
303 produced by the electrolyzer is injected to the burner, which brings another different feature between
304 the two systems. The steam power plant energy efficiency is in a reasonable range. For further
305 evaluation, the Ref (Suresh et al., 2012) is considered. The main configuration is modeled in the code.
306 The plant energy efficiency is calculated at around 29.1%, which is consistent with the plant energy
307 efficiency shown in that ref (29.3%).

308 **3.3. System energy and exergy analyses**

309 Figure 4 shows the annual average energy efficiency of various components of the system. The highest
310 and lowest energy efficiencies are related to the compressor and steam power plant.



311

312

Figure 4. Annual average energy efficiencies of various system components.

313

Figure 5 shows the annual average exergy efficiency of various components of the system. Compared with Figure 4, although the highest exergy efficiency is still related to the compressor, the lowest exergy efficiency is here related to the wind turbine.

315

316

Exergy efficiency of the burner is lower than its energy efficiency. From the exergy viewpoint, this phenomenon is due to the fact that chemical reactions usually reduce exergy efficiency and increase the exergy destruction rate. This phenomenon is also true for the electrolyzer and the methanation plant.

317

318

319

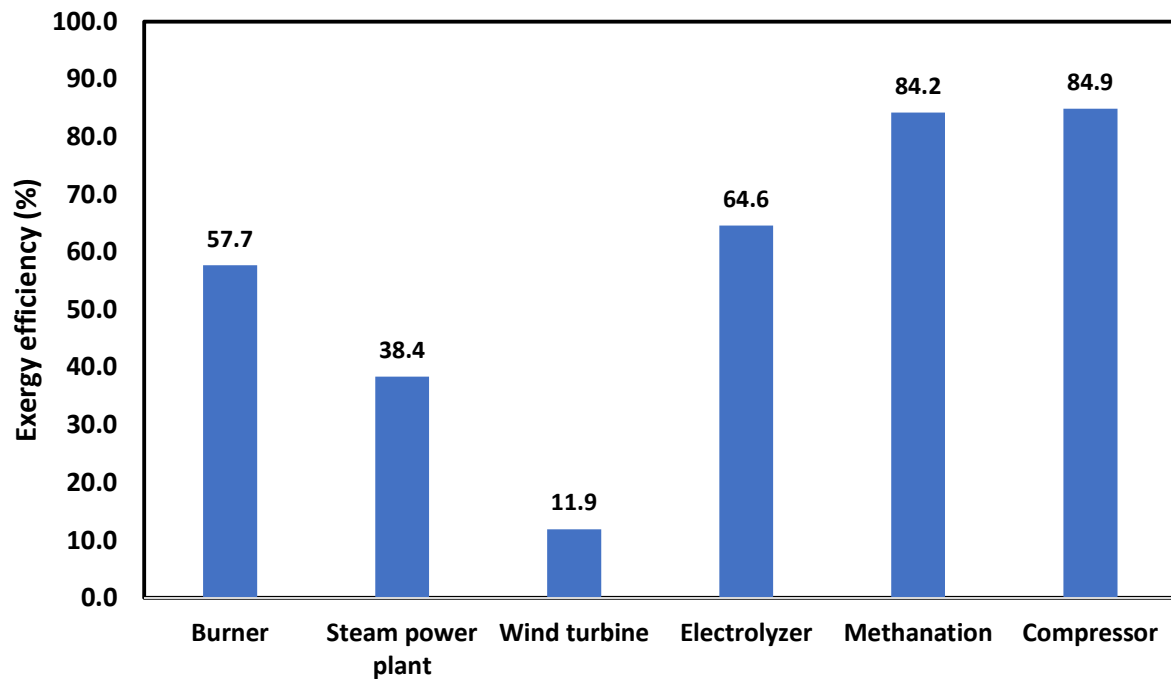
Wind turbine exergy efficiency is usually lower than wind turbine energy efficiency. The difference between energy and exergy efficiencies is because power rate of wind turbine is considered for thermal efficiency. For exergy efficiency, the exergy of wind velocity is considered (numerator of wind turbine

320

321

exergy efficiency).

322



323

324

Figure 5. Annual exergy efficiency of various system components

325

326

327

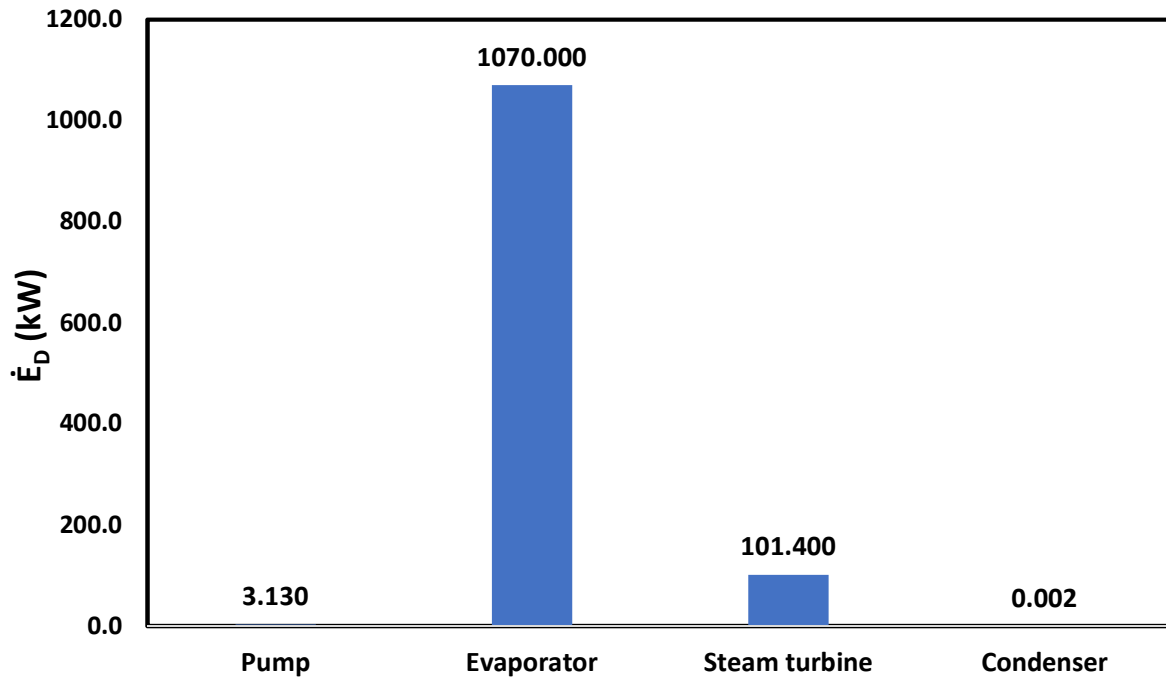
328

329

330

331

Figure 6 represents the annual average exergy destruction rate for each component of the steam power plant (Rankine cycle). The maximum exergy destruction rate is related to the evaporator because of the heat absorbed from the hot flue gas (points 3 and 4). Heat transfer is generally one of the main sources of exergy destruction. Power consumption of pumps is usually very low in the steam power plants; the exergy destruction is also low as a result. In the condenser, since heat is dissipated to the environment, exergy destruction is very low.



332

333 Figure 6. Annual average exergy destruction rate for various components of steam power plant

334 Figure 7 shows the annual average exergy destruction rate for various components of the system. The

335 maximum exergy destruction rate is related to the steam power plant which is equal to 1174.5 kW.

336 Since the steam cycle includes four components (evaporator, pump, steam turbine, and condenser) and

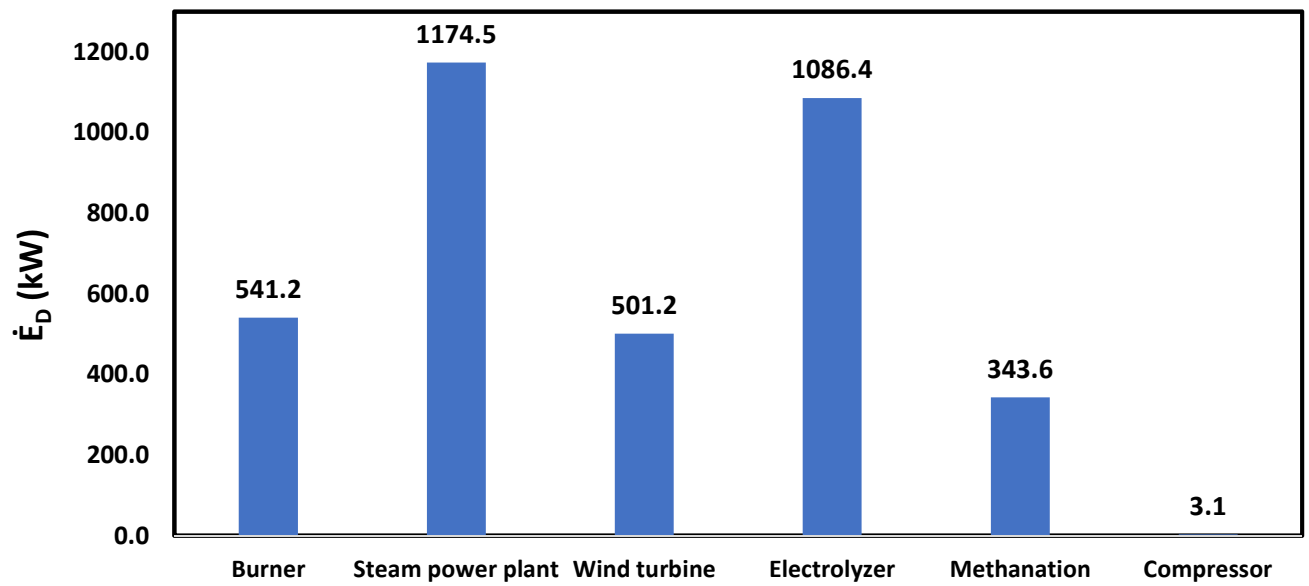
337 all of them have significant exergy destruction rates, their summation is considerable.

338 The exergy destruction rate in electrolyzer is also high (1086.4 kW) due to chemical reaction. Exergy

339 destruction in methanation and burner are considerable due to the same reason of electrolyzer.

340 The exergy destruction in one wind turbine is equal to 501.2 kW. It can be concluded that the main part

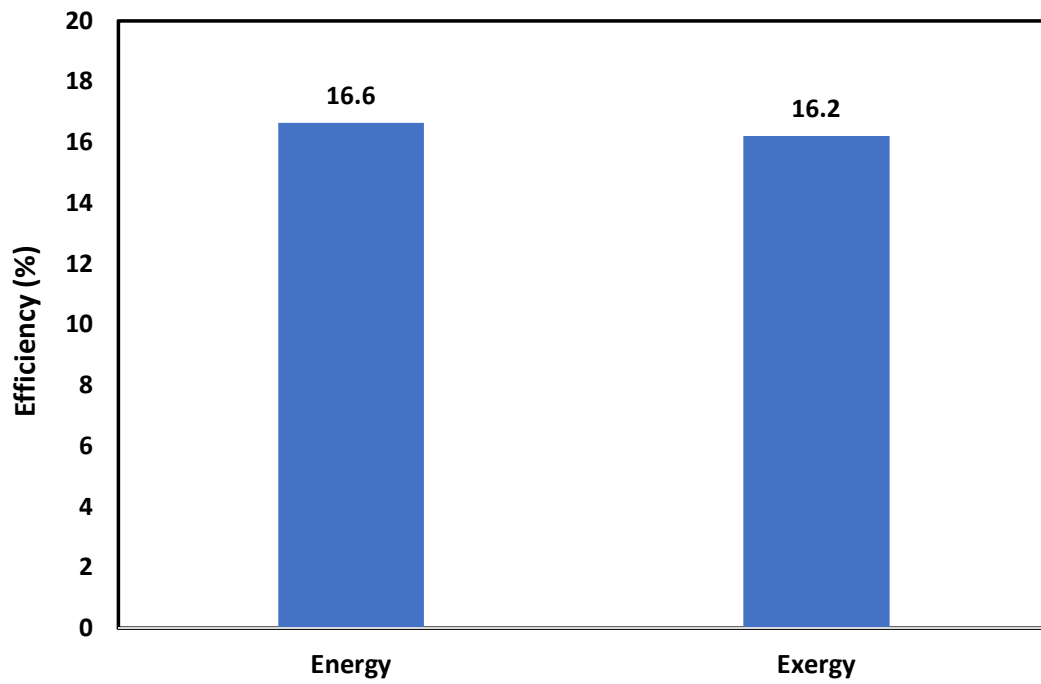
341 of wind velocity exergy is wasted in the wind turbine.



342

343 Figure 7. Annual average exergy destruction rate for various components of the system

344 Figure 8 illustrates the system energy and exergy efficiencies. Energy efficiency is slightly higher than
345 exergy efficiency. In comparison to Figure 4, it is clear that system thermal efficiency is lower than all of
346 the energy efficiencies of system components. In comparison to Figure 5, exergy efficiency of the system
347 is higher than wind turbine exergy efficiency and lower than exergy efficiency of other system
348 components.



349

350

Figure 8. System energy and exergy efficiencies

351 3.4. System economic analysis

352 Regarding the system economic analysis, the costs of coal as well as electricity, cooling, syngas and
353 carbon tax are considered according to Table 7.

354

355

356

357

358

359

360

Table 7. Cost of products and consumption of the system

No.	Products and consumptions of system	Unit	Cost	References
1	$k_{\text{electrical}}$	\$/kWh	0.22	(Bellos et al., 2019; Bellos et al., 2016; Bellos et al., 2017; Kreuter and Hofmann, 1998; Nakomčić-smaragdakis and Dragutinović, 2016; Tzivanidis et al., 2016)
2	k_{cooling}	\$/kWh	0.074	(Bellos et al., 2019; Bellos et al., 2016; Bellos et al., 2017; Kreuter and Hofmann, 1998; Nakomčić-smaragdakis and Dragutinović, 2016; Tzivanidis et al., 2016)
3	k_{CH_4}	\$/kWh	0.12	(Bellos et al., 2019; Bellos et al., 2016; Bellos et al., 2017; Kreuter and Hofmann, 1998; Nakomčić-smaragdakis and Dragutinović, 2016; Tzivanidis et al., 2016)
4	k_{Coal}	\$/t	66.58	(Guandalini et al., 2017)
5	k_{CO_2}	\$/t	31.2	(Bellos et al., 2019; Bellos et al., 2016; Bellos et al., 2017; Kreuter and Hofmann, 1998; Nakomčić-smaragdakis and Dragutinović, 2016; Tzivanidis et al., 2016)

361

362 Table 8 shows the economic investigation results for the system with and without syngas production
 363 system. Syngas production system is including electrolyzer, methanation and compressor. The PP for the
 364 system with or without syngas production are calculated to be 11.2 and 7.4 y, and this difference could
 365 be justified by considering the components required for syngas production. The NVP for the system with
 366 or without syngas production is respectively 1.6 and 8.45 US\$. The IRR index for the system with or
 367 without syngas production is 10 and 15 %.

368 Table 8. Economic investigation results for the system with and without syngas production

No.	Parameter	Unit	Values	
			With syngas	Without syngas
1	SPP	y	9.4	6.6
2	PP	y	11.2	7.4
3	IRR	%	0.1	0.15
4	NPV	US\$	1.6×10^8	8.45×10^7
5	CO	US\$	1.03×10^8	9.83×10^7
6	CF	US\$	1.09×10^7	1.49×10^7

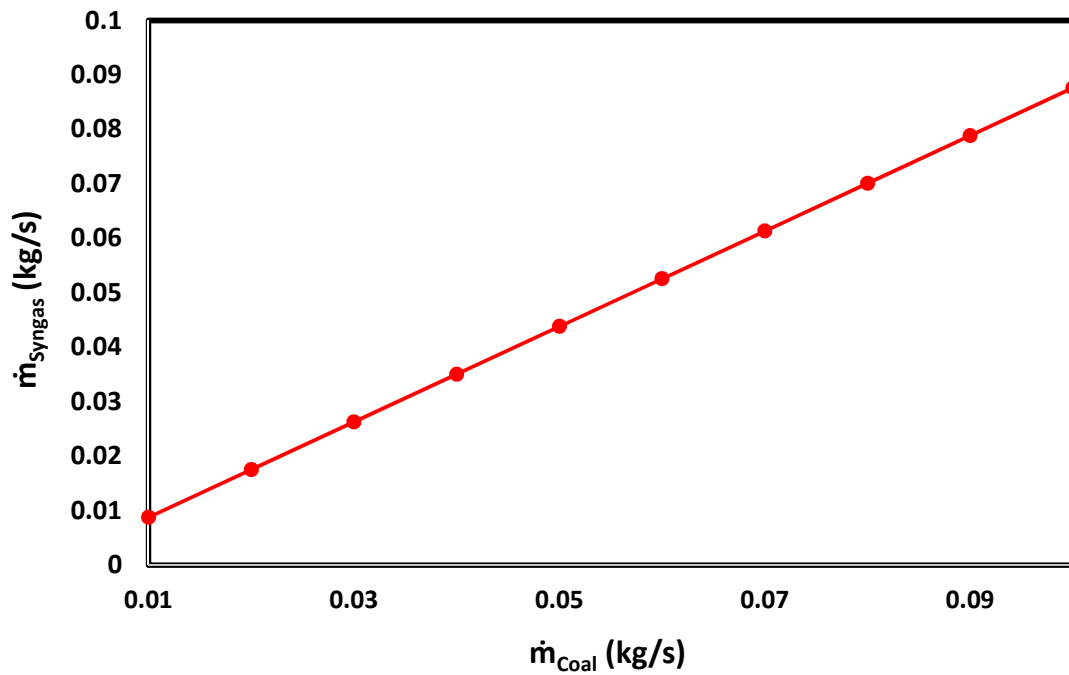
369

370 3.5. System sensitivity analysis

371 Figure 9 presents the relation between coal mass flow rate consumed by the system and syngas
 372 production. This relation is semi-linear. By changing the coal mass flow rate in the range of 0.01 to 0.1
 373 kg/s, the syngas production mass flow rate is increased from 0.009 to 0.088 kg/s. This is because CO₂
 374 production increases linearly with mass flow rate of coal and syngas production shows the same trend
 375 as CO₂ production.

376 Figure 10 shows the evolution of electrical consumption of alkaline electrolyzer as a function of coal
 377 mass flow rate burned in the burner. Similar to Figure 9, the relation is semi-linear. This is because

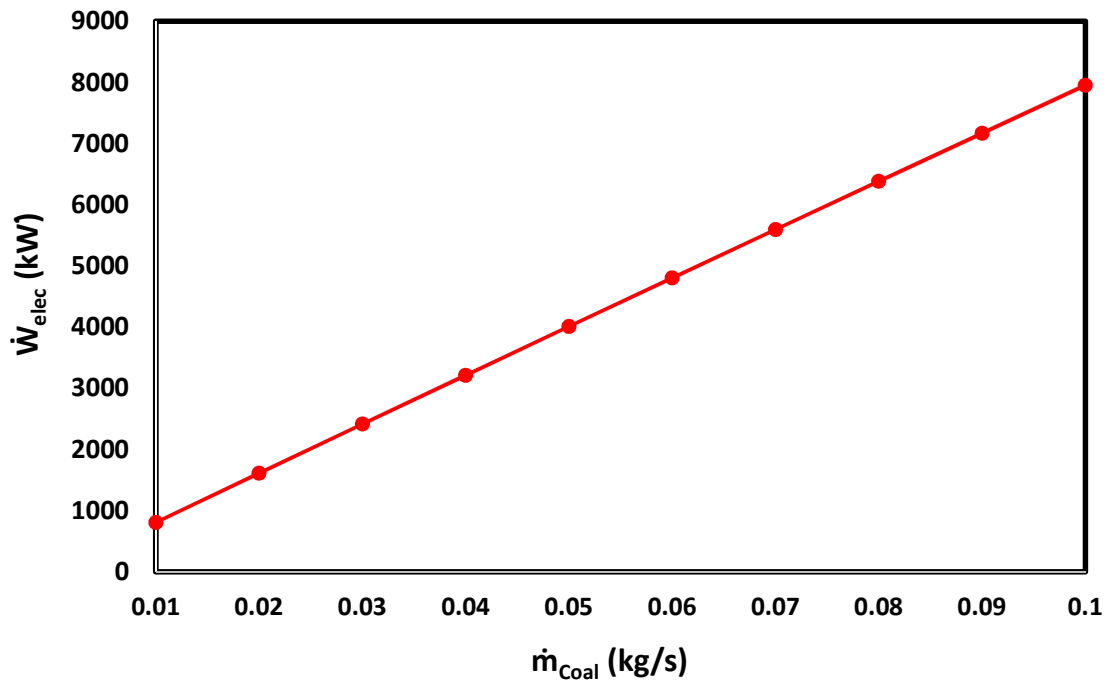
378 hydrogen need increases linearly with CO₂ production as well as coal consumption. The power
379 consumption of electrolyzer exhibits a semi-linear relationship with hydrogen production in this system.
380 It can be concluded that the electrical consumption of alkaline electrolyzer represents the highest
381 portion of system electrical consumption.



382

383

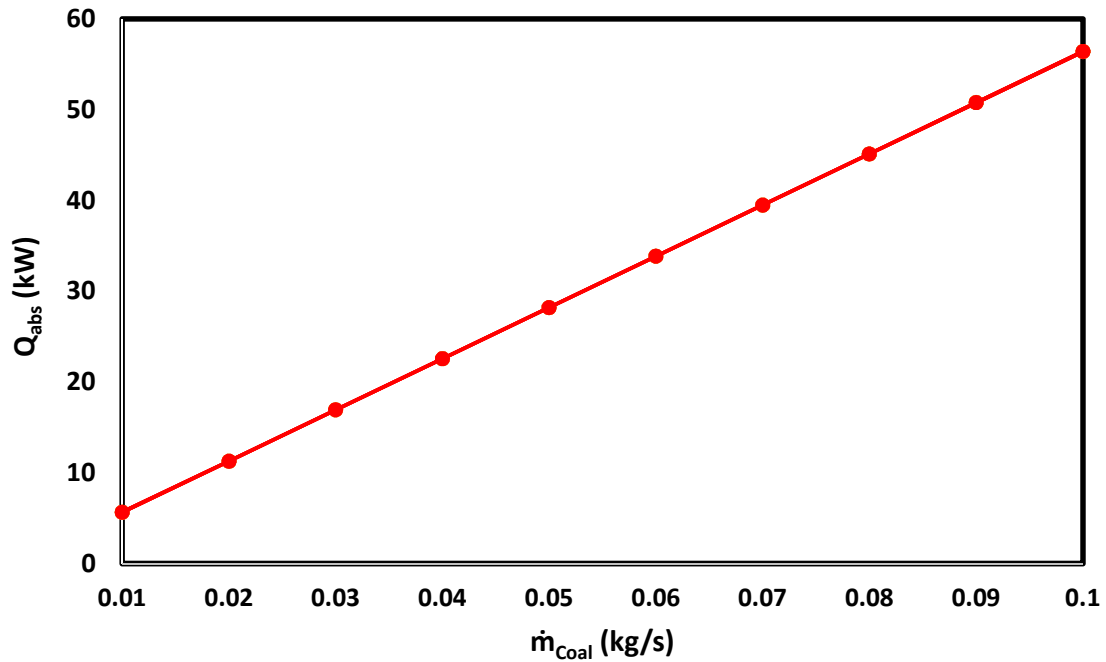
Figure 9. System syngas production versus coal mass flow rate consumption



384

385 Figure 10. Evolution of electrical consumption of alkaline electrolyzer with coal mass flow rate

386 The effect of coal mass flow rate on variation of cooling produced in absorption chiller is reported in
387 Figure 11. By increasing the coal mass flow rate in the range of 0.01 to 0.1 kg/s, the cooling produced in
388 the absorption chiller is varied from 5.6 to 56.4 kW. Increasing the coal mass flow rate generates
389 additional exhaust gas from the combustion chamber, thereby increasing the energy content of exhaust
390 gas, which in turn enhances (linear dependency) the cooling produced in the absorption chiller
391 (according to equation of absorption chiller shown in Table S1).



392

393

Figure 11. Variation of absorption chiller cooling production with coal mass flow rate

394

395

396

Figure 12 shows the system energy efficiency variation with the coal mass flow rate. The maximum system energy efficiency is reached for coal mass flow rate of 0.1 kg/s. The effect of coal mass flow rate on system energy efficiency is not considerable.

397

The following impacts on the system can be observed by increasing the coal mass flow rate:

398

399

400

401

402

- 1) According to the equation 12, by increasing the coal mass flow rate the number of wind turbines is increased to meet the electrical energy needs of electrolyzer. According to equation 13, this increase has an effect on system energy efficiency (wind turbine power production and rated power.). The system energy efficiency is decreased as a result (negative effect) due to low potential of wind in Tehran.

403

404

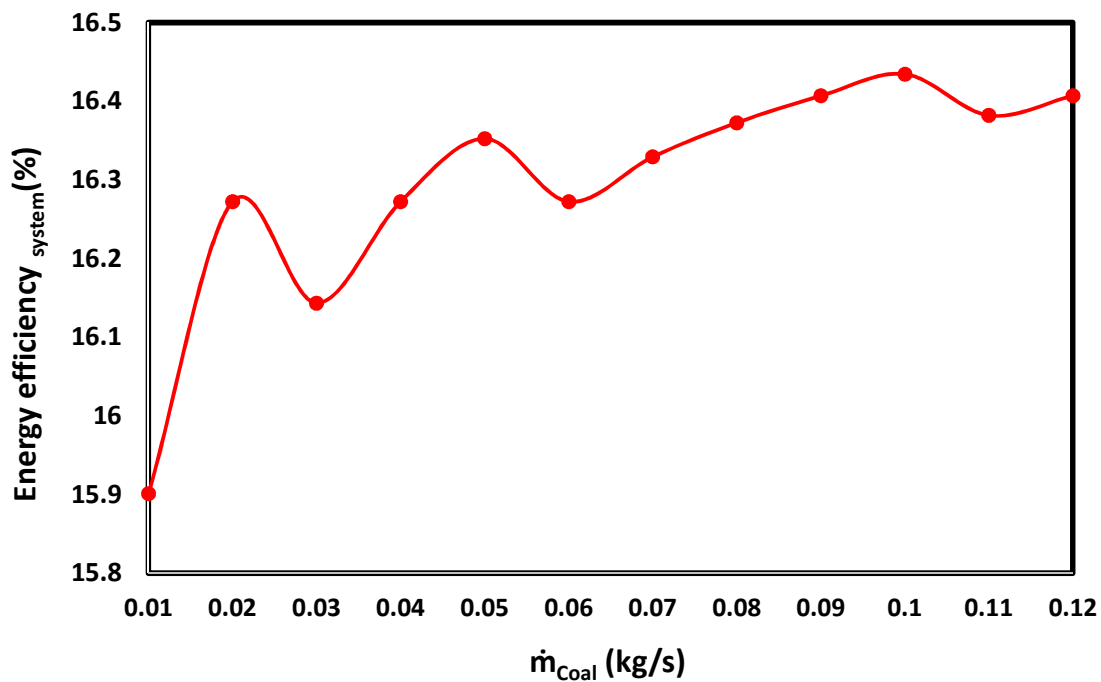
- 2) The increase of the coal mass flow rate results in the increase of the electrical power production in steam power plant and cooling production in the absorption chiller as well as syngas

405 production in methanation plant. According to equation 13, these phenomena lead to the
406 increase of system energy efficiency (positive effect).

407 3) The increase of the coal mass flow rate causes the increase of electrolyzer power consumption
408 (negative effect), since more oxygen should be produced to burn the coal in the combustion
409 chamber.

410 From the whole contribution of these effects, the optimum coal mass flow rate is identified at 0.1 kg/s.

411 Figure 13 shows the system exergy efficiency variation with changes in the coal mass flow rate. Similar
412 to Figure 12, the trend of the curve is wavy due to the same reason as for the system energy efficiency
413 behavior.

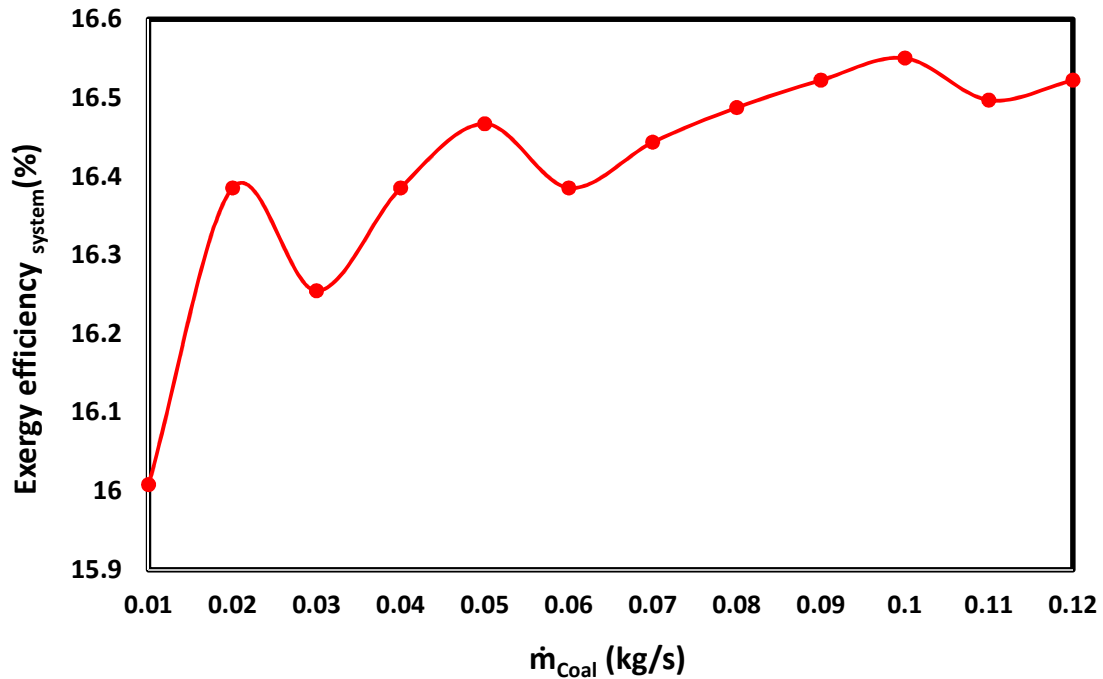


414

415 Figure 12. System energy efficiency variation with coal mass flow rate

416

417



418

419

Figure 13. System exergy efficiency variation with coal mass flow rate.

420 The changes of system exergy destruction rate with variation of coal mass flow rate are presented in

421 Figure 14. In contrast to the system energy and exergy efficiency evolutions, the trend of this curve is

422 linear. This phenomenon is due to the fact that increasing the number of wind turbines only increases

423 the exergy destruction rate. In contrast, for the system energy and exergy efficiencies, increasing the

424 number of wind turbines has an impact on both denominator and numerator of equations 13 and 15.

425 Figure 15 reveals the effect of air fuel ratio on burner energy and exergy efficiencies. By increasing air

426 fuel ratio, both the energy and exergy efficiencies of the burner are reduced. By increasing air fuel ratio,

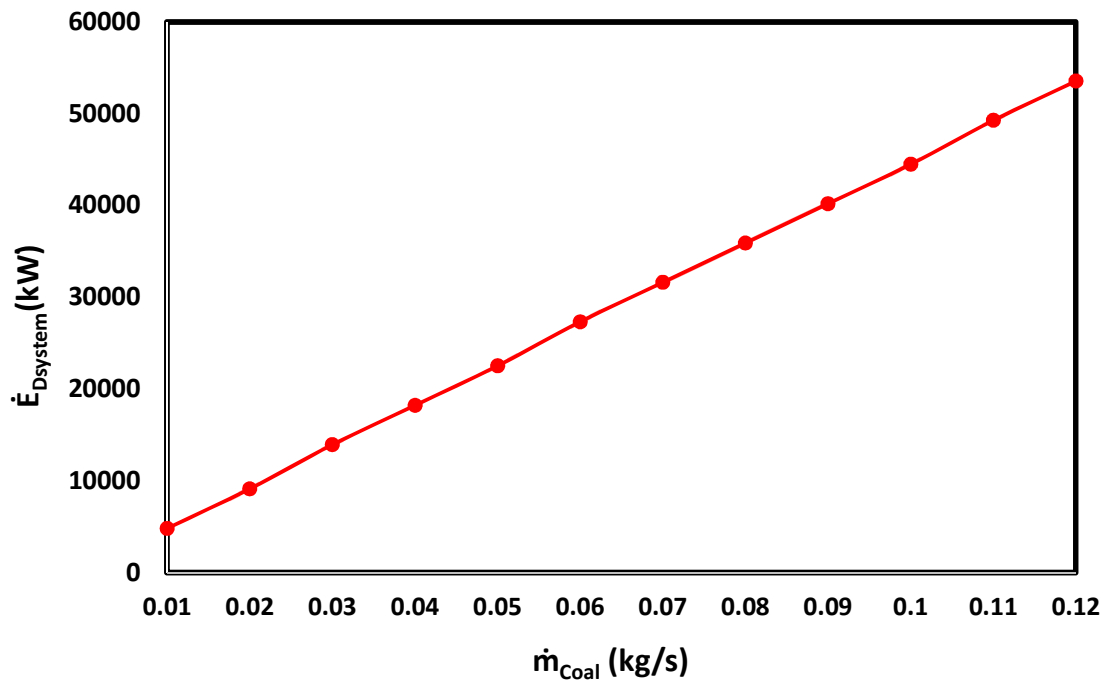
427 the exhaust gas temperature is decreased. Regarding equations in Tables S1 & S2, energy and exergy

428 efficiencies are reduced. Increasing the exhaust mass flow rate also causes an increase of the number of

429 wind turbines. This increase has a direct effect on the energy and exergy efficiencies of the system so

430 that the trend of this curve is semi linear.

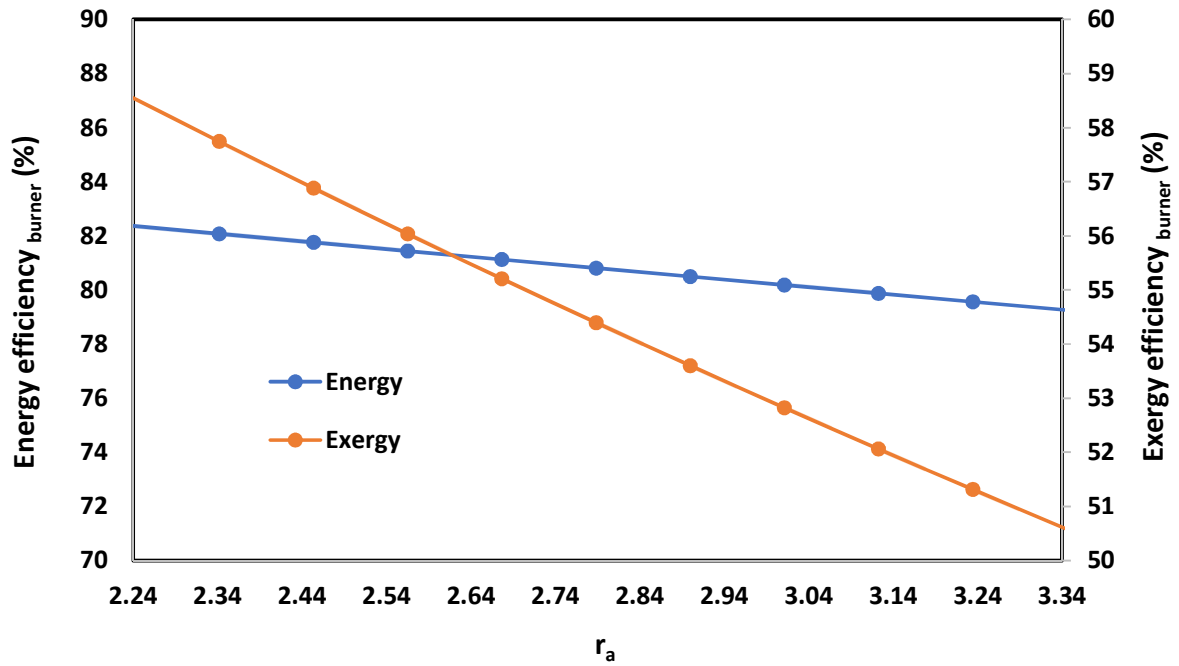
431 Figure 16 shows the exergy destruction rate of the burner with variation of air fuel ratio. As expected, by
432 increasing air fuel ratio, air mass flow rate increases. The differences between inlet and outlet exergy
433 flow rates is increased too. Since the exergy destruction is calculated based on the subtraction of inlet
434 and outlet exergy rates, the trend of this curve is semi linear.



435

436

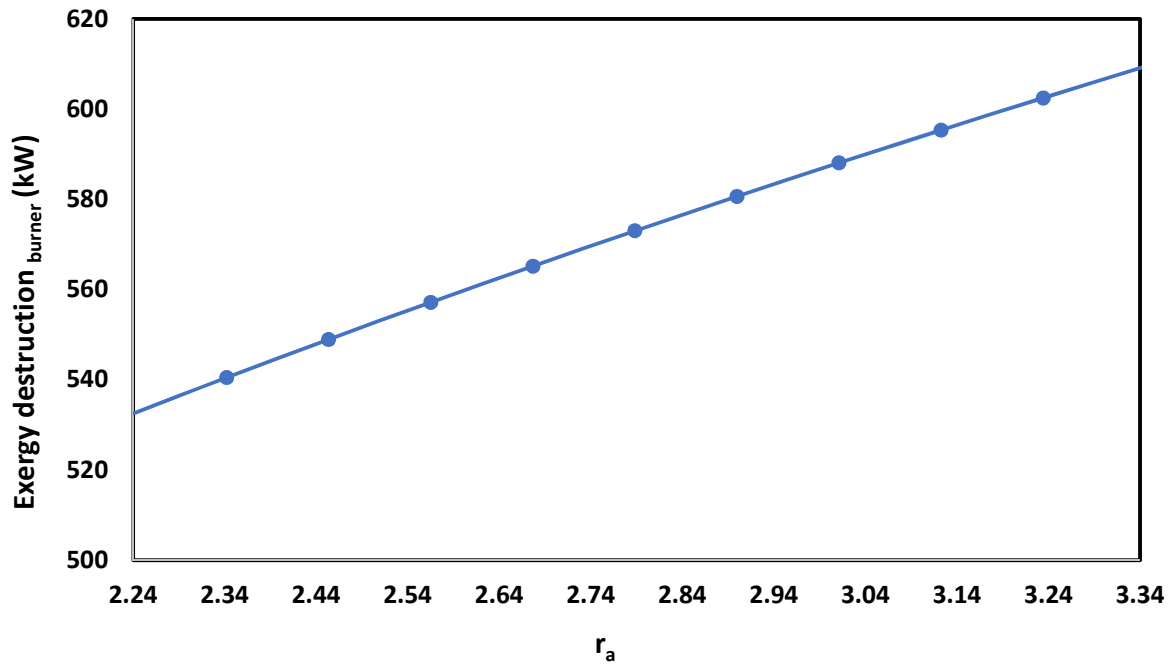
Figure 14. Effect of coal mass flow rate on system exergy destruction rate



437

438

Figure 15. Effect of air fuel ratio on burner energy and exergy efficiencies

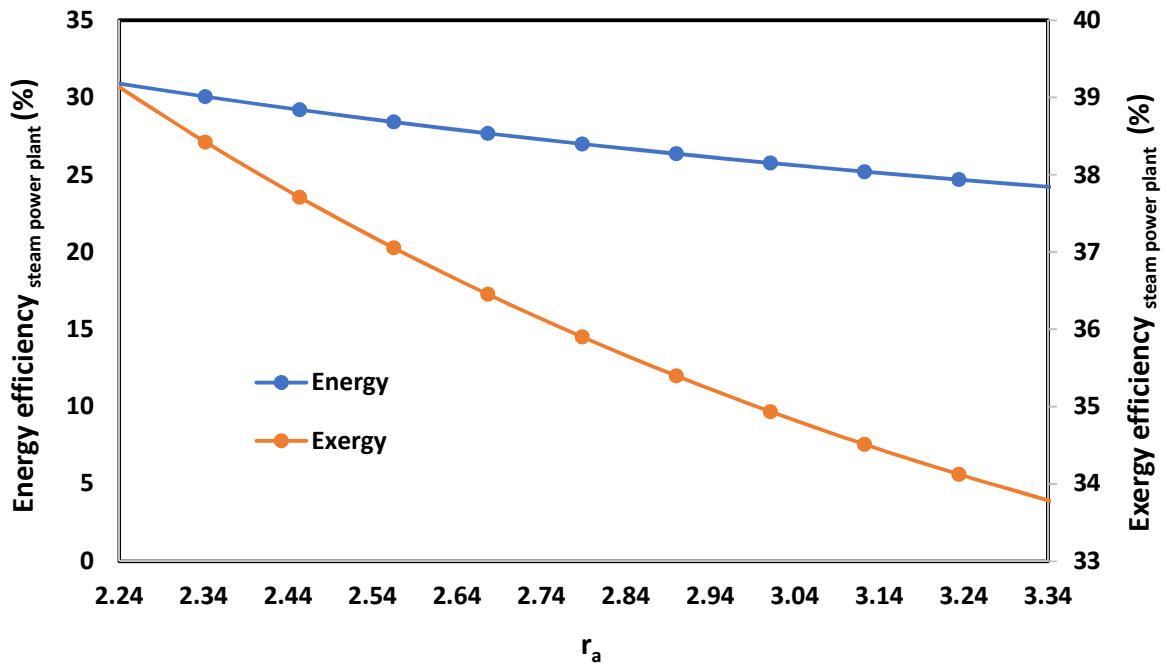


439

440

Figure 16. Effect of air fuel ratio on exergy destruction rate of the burner

441 The impact of air fuel ratio on the steam power plant (Rankine cycle) energy and exergy efficiencies is
 442 shown in Figure 17. When increasing air fuel ratio, the temperature of hot exhaust gas is decreased, the
 443 heat source temperature of the steam power plant is decreased. This decrease causes a reduction in
 444 energy and exergy efficiencies of the steam power plant.



445
 446 Figure 17. Variation of steam power plant (Rankine cycle) energy and exergy efficiencies with air fuel
 447 ratio

448 The variation of the steam power plant exergy destruction rate with changes in air fuel ratio is illustrated
 449 in Figure 18. By increasing air fuel ratio, the exhaust gas temperature is decreased. The power produced
 450 in the steam power plant as well as exergy destruction rate is decreased too.

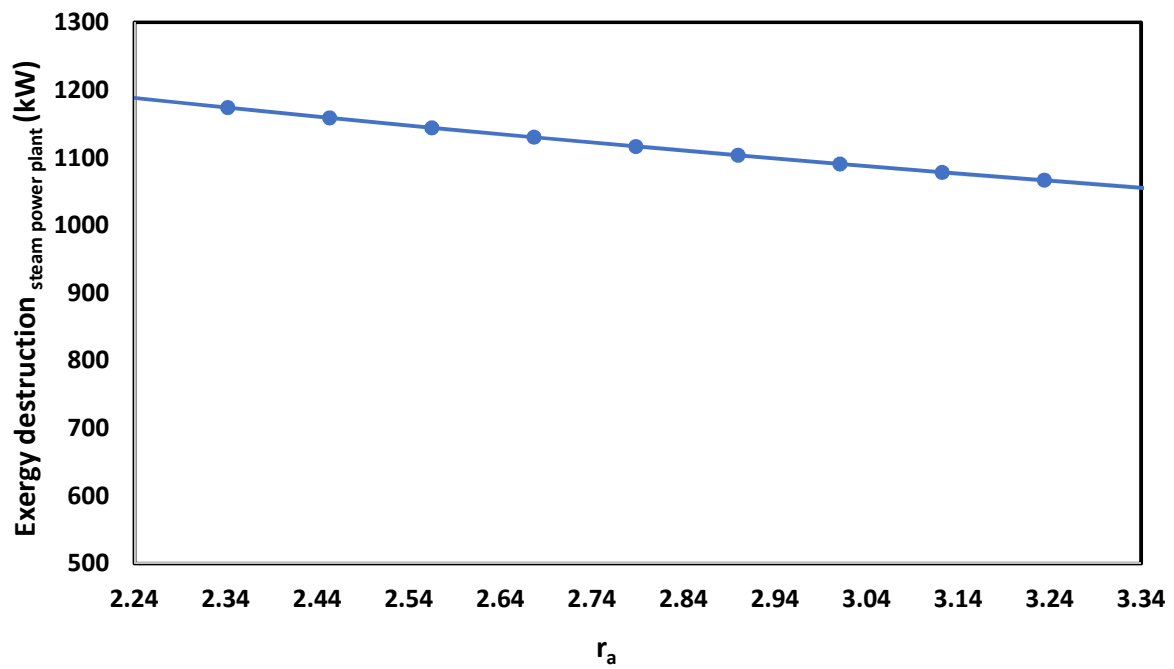
451 Figure 19 reports the effect of air fuel ratio on absorption chiller exergy destruction rate. By increasing
 452 air fuel ratio, two opposing effects can be observed:

- 453 1) Decreasing gas temperature in points 3 and 4

454 2) Increasing mass flow rates in points 3 and 4

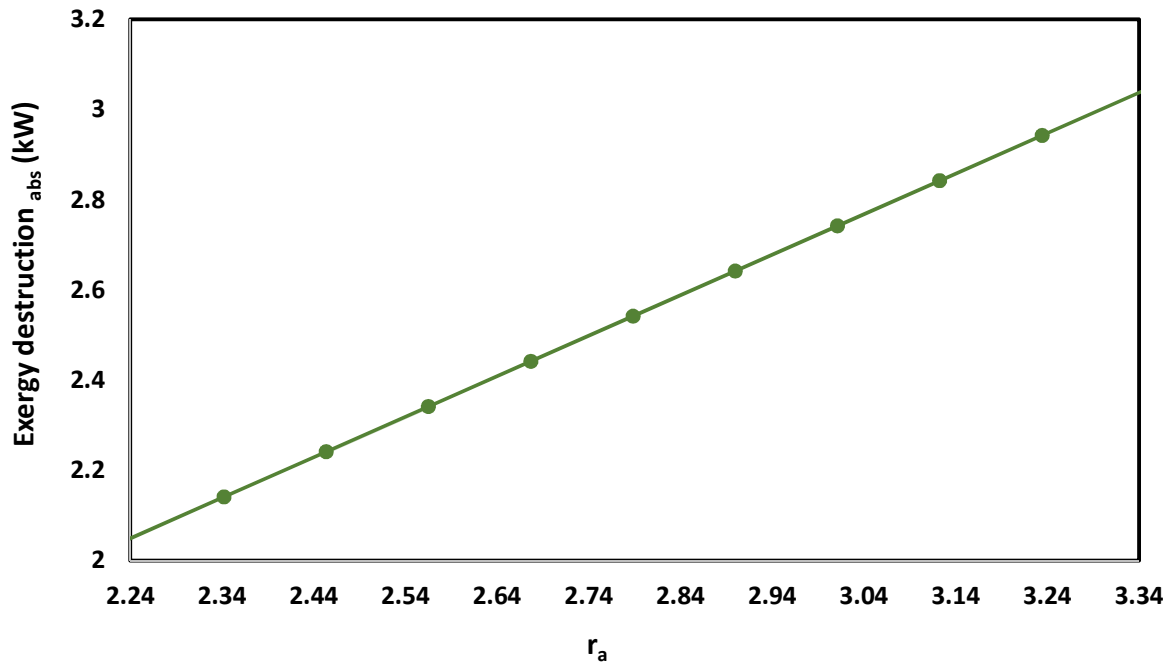
455 Although item 1 decreases the exergy destruction rate in the absorption chiller, item 2 increases this

456 value. The item 2 overcomes item 1 so that the exergy destruction rate in absorption chiller is increased.



457

458 Figure 18. Variation of steam power plant exergy destruction rate with air fuel ratio



459

460

Figure 19. Variation of absorption chiller exergy destruction rate with air fuel ratio

461 Figure 20 presents the changes of systems energy and exergy efficiencies with variation of air fuel ratio.

462 By increasing air fuel ratio, the temperature of exhaust gas is decreased too. The power production in

463 Rankine cycle is decreased as a result. By increasing the power production in Rankine cycle, the system

464 energy and exergy efficiencies are decreased, but this reduction is not considerable.

465

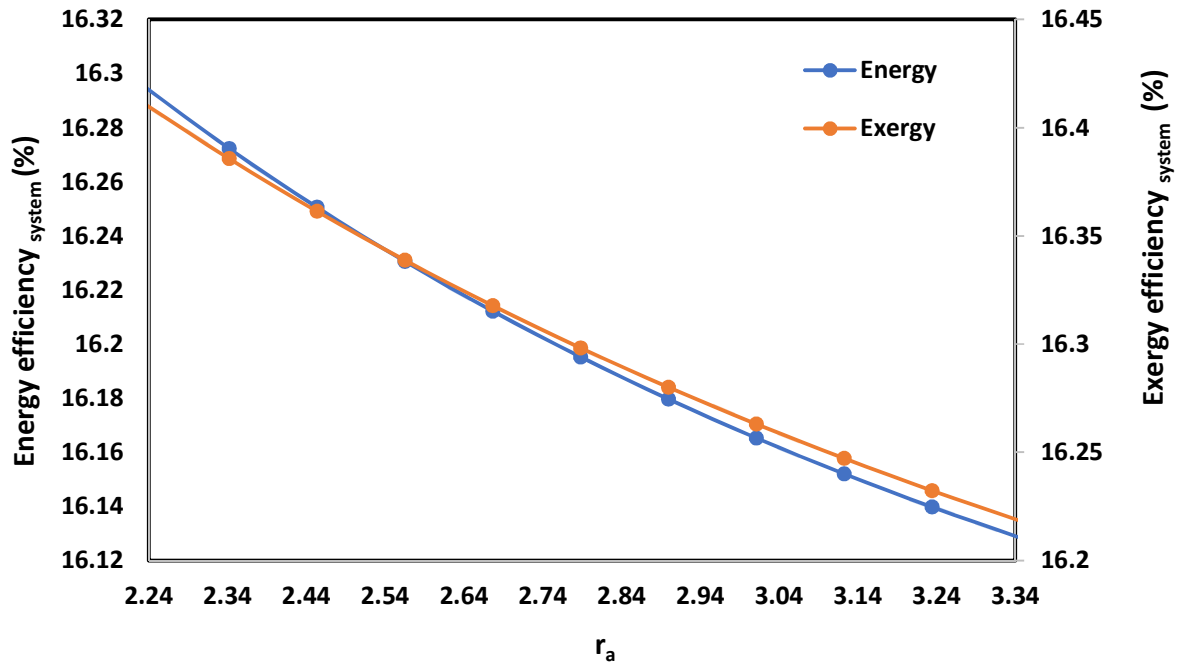


Figure 20. Variation of system energy and exergy efficiencies with air fuel ratio

4. Conclusion

In this study, a cogeneration system powered by the coal combustion chamber and wind turbines is applied to produce electricity, cooling load and syngas from the CO₂ emission of exhaust gas of the coal combustion chamber. By this way, the heat of exhaust gas of the combustion chamber runs both a Rankine cycle and an absorption chiller to generate electricity and cooling load. The exhaust gas of the combustion chamber finally flows through a sulfur extraction unit to separate sulfur from CO₂. Then, the purified CO₂ of exhaust gas reacts with hydrogen (H₂), which is produced from electrolysis of water in an electrolyzer unit. Meanwhile, the produced oxygen (O₂) from the water electrolysis process is injected into the combustion chamber to increase the efficiency of the combustion. The energy, exergy and economic analyses of this cogeneration system have been performed.

The results of this study can be summarized as follows:

The proposed system is capable of producing 1009.4 metric ton of syngas annually and it can generate 180.5 MWh of cooling load and 40920.4 MWh of electricity. This configuration produces syngas while avoiding the release of 2776 metric ton of CO₂ annually.

483 The energy efficiencies of main components consisting of methanation unit, steam power plant and
 484 wind turbine are about 85%, 30.1% and 30.7%. In the meanwhile, the exergy efficiencies for these
 485 components are 84.2%, 38.4% and 11.9%, respectively.

486 The results of this study show that the energy and exergy efficiencies of this hybrid system are 16.6%
 487 and 16.2%, respectively.

488 The economic analysis reveals that the costs of electricity generation, cooling and syngas production are
 489 0.22, 0.074, and 0.12 \$/kWh, respectively.

490 The payback periods for this hybrid system with or without syngas production are 11.2 and 7.4 years,
 491 respectively.

492 Moreover, the internal rate of return (IRR) and net present value (NPV) for this cogeneration system
 493 with syngas production unit are 10% and 1.6 US\$, respectively whereas these economic parameters for
 494 the hybrid system without syngas production unit are 15% and 8.45 US\$.

495 For further study, the application of other renewable energy resources such as solar collector or
 496 geothermal energy instead of wind turbine is suggested for this cogeneration system. This configuration
 497 can be employed to capture more CO₂ emissions from other hydrocarbon fuel combustion chambers as
 498 a future work of this study.

499 **Nomenclature**

Subscript notations

0	Reference state condition (1atm, 288K)
1, 2, ..., 15	Fifteen points in Figure 1
abs	Absorption chiller
act	Activation
Com	Compressor
C	Condenser
elec	Electrolyzer
E	Evaporator

FG	Flue gas
H	Hydrogen
ohm	Ohmic
O	Oxygen
P	Pump
rev	Reversible
S	Sulfur
T	Turbine

Variables

A	Area of electrode (m ²)
A ₂	Swept area of wind turbine (m ²)
Abs	Absorption chiller
C	Parameter of wind turbine
C ₀	Total investment cost (US\$)
CF	Cost function (\$)
COP	Coefficient of performance of absorption chiller
c _p	Specific heat at constant pressure (kJ/kgK)
ex	Total specific exergy (kJ/kg)
ex _{chi}	Component specific chemical exergy (kJ/kg)
\dot{E}_D	Exergy destruction rate
f ₁ and f ₂	Faraday efficiencies related to electrolyzer

	(mA ² /Cm ⁴)
F	Faraday`s constant (96495 C/mole)
h	Enthalpy (kJ/kg)
I	Current (A)
IRR	Internal Rate of Return
K	Parameter of wind turbine
K	Ratio (constant pressure divided to constant volume specific heat)
KK	Number of wind turbines
LHV	Lower heating value (kJ/kg)
\dot{m}	Mass flow rate (kg/s)
\dot{m}_1	\dot{m}_{coal}
\dot{m}_{15}	$\dot{m}_{\text{O}_2,\text{elec}}$
\dot{m}_2	\dot{m}_{air}
\dot{m}_3	\dot{m}_{FG}
\dot{m}_{H_2}	Hydrogen production mass flow rate in alkaline electrolyzer
N	Project lifetime equal to 25 years (y)
N_{cell}	Number of cells
NPV	Net Present Value (US\$)
PP	Payback period (y)
O ₂ , elec	Oxygen produced in the electrolyzer
P_{er}	Rated power of wind turbine (kW)

\dot{Q}	Heat transfer rate (kW)
r_1 and r_2	Ohmic resistance parameters (Ωm^2)
r_a	Air fuel ratio
r_c	Compressor pressure ratio
R	specific gas constant (kJ/kgK)
RC	Rankine cycle
R_i	Specific gas constant (kJ/kgK)
r	Discount factor equal to 3%
s	Specific entropy (kJ/kgK)
SPP	Simple Payback Period (y)
t_1, t_2 and t_3	electrode overvoltage coefficients (m^2/A)
T	Temperature (K)
T_1	T_{coal} (K)
T_{15}	$T_{O_2,elec}$ (K)
T_2	T_{air} (K)
T_3	T_{FG} (K)
u	Wind velocity (m/s)
\bar{u}	Average wind speed (m/s)
u_c	Cut-in speed (m/s)
u_r	Rated speed (m/s)
u_f	Furling speed (m/s)
V	Operating voltage (V)
V_{cell}	Voltage of cells (V)

\dot{W}	Power transfer rate (kW)
\dot{W}_c	Consumption power in the compressor (kW)
\dot{W}_{elec}	Consumption power in alkaline electrolyzer (kW)
$\dot{W}_{wind,ave}$	Average electrical power generated by wind (kW) turbine
x	Weight fraction
x_1	x_{coal}
x_{15}	$x_{O_2,elec}$
x_2	x_{air}
x_3	x_{FG}
σ	Standard deviation
ρ	Air density (kg/m ³)
η_c	Condenser heat transfer efficiency
η_E	Evaporator heat transfer efficiency
η_{CB}	Combustion loss efficiency
η_{Com}	Polytrophic compressor efficiency
η_F	Current efficiency of alkaline electrolyzer
η_P	Pump polytrophic efficiency
η_T	Turbine polytrophic efficiency
ΔG	Gibbs energy (equal to 237.2 kJ/mol)
Γ	Gamma function

500

501 **References**

- 502 Ahmadi, A., Jamali, D., Ehyaei, M., Assad, M. E. H., 2020. Energy, Exergy, Economic and
 503 Exergoenvironmental analyses of gas and air bottoming cycles for production of electricity and
 504 hydrogen with gas reformer. *Journal of Cleaner Production*. 120915.
- 505 Anderson, B., 2015. Coal Fired Boiler-Principle 2. Seminar on Coal Fired Boiler, Malaysia.
- 506 Atabi, F., Ehyaei, M. A., Ahmadi, M. H. (2014). *Calculation of CH₄ and CO₂ emission rate in Kahrizak*
 507 *landfill site with LandGEM mathematical model*. Paper presented at the The 4th world
 508 sustainability forum.
- 509 Bailera, M., Lisbona, P., Romeo, L. M., 2015. Power to gas-oxyfuel boiler hybrid systems. *International*
 510 *Journal of Hydrogen Energy*. 40(32), 10168-75.
- 511 Bailera, M., Lisbona, P., Romeo, L. M., Espatolero, S., 2016. Power to Gas–biomass oxycombustion hybrid
 512 system: Energy integration and potential applications. *Applied energy*. 167, 221-29.
- 513 Bejan, A., 2016. *Advanced engineering thermodynamics*. John Wiley & Sons
- 514 Bellocchi, S., De Falco, M., Gambini, M., Manno, M., Stilo, T., Vellini, M., 2019. Opportunities for power-
 515 to-Gas and Power-to-liquid in CO₂-reduced energy scenarios: The Italian case. *Energy*.
- 516 Bellos, E., Pavlovic, S., Stefanovic, V., Tzivanidis, C., Nakomcic-Smaradgakis, B. B., 2019. Parametric
 517 analysis and yearly performance of a trigeneration system driven by solar-dish collectors.
 518 *International Journal of Energy Research*. 43(4), 1534-46.
- 519 Bellos, E., Tzivanidis, C., Antonopoulos, K. A., 2016. Exergetic, energetic and financial evaluation of a solar
 520 driven absorption cooling system with various collector types. *Applied Thermal Engineering*.
 521 102, 749-59.
- 522 Bellos, E., Tzivanidis, C., Symeou, C., Antonopoulos, K. A., 2017. Energetic, exergetic and financial
 523 evaluation of a solar driven absorption chiller–A dynamic approach. *Energy conversion and*
 524 *management*. 137, 34-48.
- 525 Boubenia, A., Hafaifa, A., Kouzou, A., Mohammedi, K., Becherif, M., 2017. Carbone dioxide capture and
 526 utilization in gas turbine plants via the integration of power to gas. *Petroleum*. 3(1), 127-37.
- 527 Buttler, A., Spliethoff, H., 2018. Current status of water electrolysis for energy storage, grid balancing and
 528 sector coupling via power-to-gas and power-to-liquids: A review. *Renewable and Sustainable*
 529 *Energy Reviews*. 82, 2440-54.
- 530 Castaneda, M., Cano, A., Jurado, F., Sánchez, H., Fernandez, L. M., 2013. Sizing optimization, dynamic
 531 modeling and energy management strategies of a stand-alone PV/hydrogen/battery-based
 532 hybrid system. *International journal of hydrogen energy*. 38(10), 3830-45.
- 533 Conti, J., Holtberg, P., Diefenderfer, J., LaRose, A., Turnure, J. T., Westfall, L. (2016). *International energy*
 534 *outlook 2016 with projections to 2040: USDOE Energy Information Administration (EIA)*,
 535 Washington, DC (United States
- 536 De Santoli, L., Basso, G. L., Nastasi, B., 2017. The potential of hydrogen enriched natural gas deriving
 537 from power-to-gas option in building energy retrofitting. *Energy and Buildings*. 149, 424-36.
- 538 Dorotić, H., Doračić, B., Dobravec, V., Pukšec, T., Krajačić, G., Duić, N., 2019. Integration of transport and
 539 energy sectors in island communities with 100% intermittent renewable energy sources.
 540 *Renewable and Sustainable Energy Reviews*. 99, 109-24.
- 541 García–García, I., Barrio, V., Cambra, J., 2018. Power-to-Gas: Storing surplus electrical energy. Study of
 542 catalyst synthesis and operating conditions. *International Journal of Hydrogen Energy*. 43(37),
 543 17737-47.
- 544 Ghaib, K., Ben-Fares, F.-Z., 2018. Power-to-Methane: A state-of-the-art review. *Renewable and*
 545 *Sustainable Energy Reviews*. 81, 433-46.
- 546 Gholizadeh, N., Vahid-Pakdel, M., Mohammadi-ivatloo, B., 2019. Enhancement of demand supply's
 547 security using power to gas technology in networked energy hubs. *International Journal of*
 548 *Electrical Power & Energy Systems*. 109, 83-94.

- 549 Gondal, I. A., 2019. Hydrogen integration in power-to-gas networks. *International Journal of Hydrogen*
550 *Energy*. 44(3), 1803-15.
- 551 Guandalini, G., Robinius, M., Grube, T., Campanari, S., Stolten, D., 2017. Long-term power-to-gas
552 potential from wind and solar power: A country analysis for Italy. *International Journal of*
553 *Hydrogen Energy*. 42(19), 13389-406.
- 554 Iaquaniello, G., Setini, S., Salladini, A., De Falco, M., 2018. CO₂ valorization through direct methanation of
555 flue gas and renewable hydrogen: A technical and economic assessment. *International Journal*
556 *of Hydrogen Energy*. 43(36), 17069-81.
- 557 Jamali, D. H., Noorpoor, A., 2019. Optimization of a novel solar-based multi-generation system for waste
558 heat recovery in a cement plant. *Journal of Cleaner Production*. 240, 117825.
- 559 Johnson, G. L., 2006. *Wind energy systems*. Citeseer
- 560 Justus, C. G., 1978. *Winds and wind system performance*. Research supported by the National Science
561 Foundation and Energy Research and Development Administration. Philadelphia, Pa., Franklin
562 Institute Press, 1978. 120 p.
- 563 Kirchbacher, F., Biegger, P., Miltner, M., Lehner, M., Harasek, M., 2018. A new methanation and
564 membrane based power-to-gas process for the direct integration of raw biogas—Feasibility and
565 comparison. *Energy*. 146, 34-46.
- 566 Kreuter, W., Hofmann, H., 1998. Electrolysis: the important energy transformer in a world of sustainable
567 energy. *International Journal of Hydrogen Energy*. 23(8), 661-66.
- 568 Lewandowska-Bernat, A., Desideri, U., 2018. Opportunities of power-to-gas technology in different
569 energy systems architectures. *Applied energy*. 228, 57-67.
- 570 Li, Z. X., Ehyaei, M. A., Kamran Kasmaei, H., Ahmadi, A., Costa, V., 2019. Thermodynamic modeling of a
571 novel solar powered quad generation system to meet electrical and thermal loads of residential
572 building and syngas production. *Energy Conversion and Management*. 199, 111982.
- 573 Lisbona, P., Frate, G. F., Bailera, M., Desideri, U., 2018. Power-to-Gas: Analysis of potential
574 decarbonization of Spanish electrical system in long-term prospective. *Energy*. 159, 656-68.
- 575 Llera, E., Romeo, L., Bailera, M., Osorio, J., Ebro, C. R., de Luna, M., 2018. Exploring the integration of the
576 power to gas technologies and the sustainable transport. *Towards Energy Sustain*. 77.
- 577 Miao, B., Chan, S. H., 2019. The economic feasibility study of a 100-MW Power-to-Gas plant.
578 *International Journal of Hydrogen Energy*.
- 579 Mozafari, A., Ehyaei, M. A., 2012. Effects of Regeneration Heat Exchanger on Entropy, Electricity Cost,
580 and Environmental Pollution Produced by Micro Gas Turbine System. *International Journal of*
581 *Green Energy*. 9(1), 51-70.
- 582 Nakomčić-smaragdakis, B. B., Dragutinović, N. G., 2016. HYBRID RENEWABLE ENERGY SYSTEM
583 APPLICATION FOR ELECTRICITY AND HEAT SUPPLY OF A RESIDENTIAL BUILDING. *Thermal*
584 *Science*. 20(2).
- 585 Pierrot, M., 2019. The wind power database. See www.thewindpower.net.
- 586 Powell, W. R., 1981. An analytical expression for the average output power of a wind machine. *Solar*
587 *Energy*. 26(1), 77-80.
- 588 Roadmap, E. (2011). *Mapping renewable energy pathways towards 2020: EREC*.
- 589 Schaaf, T., Grünig, J., Schuster, M. R., Rothenfluh, T., Orth, A., 2014. Methanation of CO₂-storage of
590 renewable energy in a gas distribution system. *Energy, Sustainability and Society*. 4(1), 2.
- 591 Shaygan, M., Ehyaei, M. A., Ahmadi, A., Assad, M. E. H., Silveira, J. L., 2019. Energy, exergy, advanced
592 exergy and economic analyses of hybrid polymer electrolyte membrane (PEM) fuel cell and
593 photovoltaic cells to produce hydrogen and electricity. *Journal of Cleaner Production*. 234, 1082-
594 93.

- 595 Shirmohammadi, R., Soltanieh, M., Romeo, L. M., 2018. Thermo-economic analysis and optimization of
596 post-combustion CO₂ recovery unit utilizing absorption refrigeration system for a natural-gas-
597 fired power plant. *Environmental Progress & Sustainable Energy*. 37(3), 1075-84.
- 598 Suresh, M., Reddy, K., Kolar, A., 2012. Thermodynamic analysis of a coal-fired power plant repowered
599 with pressurized pulverized coal combustion. *Proceedings of the Institution of Mechanical
600 Engineers, Part A: Journal of Power and Energy*. 226(1), 5-16.
- 601 Thema, M., Bauer, F., Sterner, M., 2019. Power-to-Gas: Electrolysis and methanation status review.
602 *Renewable and Sustainable Energy Reviews*. 112, 775-87.
- 603 Tijani, A. S., Yusup, N. A. B., Rahim, A. H. A., 2014. Mathematical Modelling and Simulation Analysis of
604 Advanced Alkaline Electrolyzer System for Hydrogen Production. *Procedia Technology*. 15, 798-
605 806.
- 606 Toro, C., Sciubba, E., 2018. Sabatier based power-to-gas system: Heat exchange network design and
607 thermo-economic analysis. *Applied energy*. 229, 1181-90.
- 608 Tzivanidis, C., Bellos, E., Antonopoulos, K. A., 2016. Energetic and financial investigation of a stand-alone
609 solar-thermal Organic Rankine Cycle power plant. *Energy conversion and management*. 126,
610 421-33.
- 611 Ulleberg, Ø., 2003. Modeling of advanced alkaline electrolyzers: a system simulation approach.
612 *International Journal of Hydrogen Energy*. 28(1), 21-33.
- 613 Verma, A., Singh, T., Monjezi, M., 2010. Intelligent prediction of heating value of coal. *Iranian Journal of
614 Earth Sciences*. 2, 32-38.
- 615 Walker, S. B., van Lanen, D., Mukherjee, U., Fowler, M., 2017. Greenhouse gas emissions reductions from
616 applications of Power-to-Gas in power generation. *Sustainable Energy Technologies and
617 Assessments*. 20, 25-32.
- 618 Weidner, S., Faltenbacher, M., François, I., Thomas, D., Skúlason, J., Maggi, C., 2018. Feasibility study of
619 large scale hydrogen power-to-gas applications and cost of the systems evolving with scaling up
620 in Germany, Belgium and Iceland. *International Journal of Hydrogen Energy*. 43(33), 15625-38.
- 621 Wulf, C., Linßen, J., Zapp, P., 2018. Review of power-to-gas projects in Europe. *Energy Procedia*. 155,
622 367-78.
- 623 Yang, Y., Guo, S., Liu, D., Li, R., Chu, Y., 2018. Operation optimization strategy for wind-concentrated
624 solar power hybrid power generation system. *Energy conversion and management*. 160, 243-50.
- 625
- 626
- 627
- 628
-

Research highlights

- A novel configuration of coal-fired cogeneration hybrid plant is proposed
- The system is powered by both the coal combustion chamber and wind turbines
- The process uses wind energy and co-produces electricity, cooling load and syngas
- CO₂ emissions in exhaust gas are reduced by conversion to syngas in methanation unit
- Energy, exergy and economic analyses of this hybrid generation system are performed

Journal Pre-proof

Author contribution section

The contribution of all authors for the paper entitled” **Energy, exergy and economic analyses of new coal-fired cogeneration hybrid plant with wind energy resource**

are the same.

Corresponding author

M.A.Ehyaei

Journal Pre-proof

Declaration of interests

The authors declare that they have no known competing financial interests or personal relationships that could have appeared to influence the work reported in this paper.

The authors declare the following financial interests/personal relationships which may be considered as potential competing interests:

M.A.Ehyaei
Corresponding author

Journal Pre-proof